STUDIA UNIVERSITATIS
BABEŞ-BOLYAI

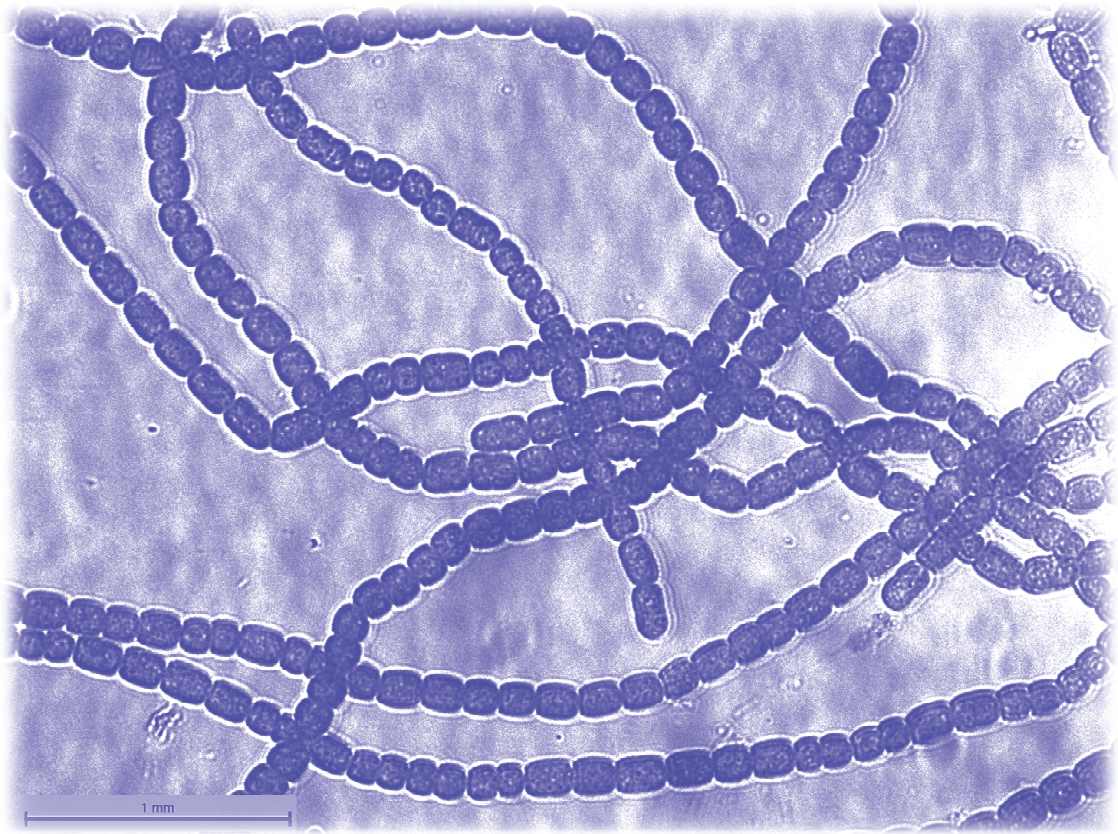

BIOLOGIA

2/2012

STUDIA
UNIVERSITATIS BABEŞ-BOLYAI

BIOLOGIA

2 / 2012
July – December

EDITORIAL BOARD
STUDIA UNIVERSITATIS BABEŞ-BOLYAI
BIOLOGIA

YEAR **2012**
VOLUME **57 (LVII)**
MONTH **DECEMBER**
ISSUE **2**

S T U D I A
UNIVERSITATIS BABEŞ-BOLYAI
BIOLOGIA

2

EDITORIAL OFFICE: M. Kogălniceanu 1 • 400084 Cluj-Napoca • Phone: 0264 405300

SUMAR – CONTENTS – SOMMAIRE – INHALT

All authors are responsible for submitting manuscripts in comprehensible US or UK English and ensuring scientific accuracy.

Original picture on front cover:

Microscopic view of the filamentous cyanobacterium *Anabaena* strain ATCC29413

STUDIA UBB BIOLOGIA, LVII, 2, 2012 (p. 5-13)

PREDICTION OF VEGETATION DYNAMICS ON THE TAILING DUMPS IN CĂPUŞ AND AGHIREŞ (CLUJ COUNTY) BASED ON THE RESEARCHES PERFORMED DURING THE 2005 – 2011 PERIOD

SABINA TOT[1] and SILVIA OROIAN[2] ✉

SUMMARY: The paper presents the floristic structure of the nodal phytocenoses identified in the vegetation dynamics on the tailing dumps from Căpuş and Aghireş (Cluj County). The incipient vegetation phase of the tailing dumps, regardless of the chemical nature of the stored tailings, is represented by the *Tussilago farfara* phytocenoses. Within the following phase, when certain Poacee species begin to grown on the tailings, the phytocenoses succession is different. On the acid tailing dumps, one may notice the *Calamagrostis epigejos* and the *Festuca rubra* phytocenoses with *Agrostis capillaris*, while on the neutral or alkaline reaction tailing dumps the *Elymus repens* and *Festuca rupicola* phytocenoses are installed. These phytocenoses keep their individuality until the populations of some arbuscular species present in their structure, become prevalent. Within the current study, the *Crataegus monogyna* and *Prunus spinosa* phytocenoses end the succession of herbal phytocenoses and enable the growth of forest phytocenoses by the created microclimate.

Keywords: tailing dumps, phytocenoses, vegetation succession.

[1] *Waldorf High school, Cluj-Napoca, S. Celibidache Str. No. 8-12, E-mail: totsabina@gmail.com*

[2] ✉ ***Corresponding author**: **Silvia Oroian**, Department of Pharmaceutical Botany and Cell Biology, Faculty of Pharmacy, University of Medicine and Pharmacy, Gh. Marinescu Street No. 38, Târgu-Mureş, RO-540139, Romania. E-mail: osilvia@umftgm.ro*

Introduction

The two tailing dumps were formed due to the economic activities developed in this region for the valorization of mineral substances used in the industry. The tailing dumps from Căpuş developed as a result of tailing deposition during the 1969 – 1975 period, pursuant to the processing of the iron ore mined from the North-Eastern side of the Gilău Mountains. The tailing dumps from Aghireş were formed as a result of kaolin exploitation in the Northern part of the Dumbrava locality (Pop, 2001, 2007). The tailing dumps in Căpuş, located at 540-590 m.s.m. are 20 – 25 years old and they have a clay-sandy-rocky structure, forming an acid reaction technogenous soil, while the tailing dumps in Aghireş, located at of 450-480 m elevation, are 20-25 years old, with a sandy-clayey structure, and a weak-alkaline or neutral reaction.

The vegetal communities developed on the two types of tailing dumps have followed a partially different dynamics.

Materials and methods

The research of the vegetation dynamics on the tailing dumps employed the inventory squares method (Anghel *et al*., 1971, Cristea *et al.*, 2004) and the method of the phytocenological surveys.

In order to grasp the evolution of the vegetation dynamics, the authors have performed quantitative field measurements, by means of the metric frame, in 120 inventory squares and have performed 292 phytocenological surveys on the tailing dumps in Căpuş and Aghireş, under various vegetation stages.

Figure 1. Tussilaginetum farfarae on Western slope of sampled site.

Results and discussions

The floristic composition of phytocenoses installed on the tailing dumps differ depending on the nature of the exploited geologic substrata and on the duration of the deposits formation.

Within the first stage of plant colonization, regardless of the geological structure, the *Tussilago farfara* phytocenoses accommodate. Their structure includes the following species: *Leontodon autumnalis, Convolvulus arvensis, Cirsium arvense, Setaria viridis, Trifolium repens, Polygonum persicaria, Poa compressa, Sonchus arvensis* (Table 1, column 1).

The second stage, consisting in tailing colonization, begins with the occurrence of some species of Poacee perene. These are installed on the tailings sections where some of the exceeding elements (Fe, Al, K_2O, Mg, S) are leached. Starting with this stage, the dynamic evolution of the phytocenoses differs in relation to the physico-chemical and nutritional properties of the soil layer.

The *Tussilago farfara* pioneer communities developed on the tailing dumps in Căpuş, whose reaction was mainly acid, due to the high content of SiO_2, Al_2O_3 and FeO (Despu, 1985), were followed mainly by the *Calamagrostis epigejos* oligotrophic phytocenoses. Together with this species, which covers 25-35% on average, highly present are the following species: *Agrostis capillaris, Daucus carota* ssp. *carota, Plantago lanceolata, Cynosurus cristatus, Agrimonia eupatoria* and *Centaurium pulchellum* (Table 1, column 2a). In a few years (5-6), when the tailing dump begins to turn into soil and when more nutrient substances accumulate at the bottom, representative substances develop, presenting some mesophile and mesothophic pastures phytocenoses. The prevailing plant species in these phytocenoses are*: Phleum pratense, Arrhenatherum elatius* and *Dactylis glomerata,* which cover together 35-45% (Table 1, column 4a). Beside these, the following species are frequently met: *Agrostis capillaris, Daucus carota* ssp. *carota, Cynosurus cristatus, Achillea millefolium, Briza media, Centaurea nigrescens, Geranium pratense, Medicago falcata, Trifolium pratense, Trisetum flavescens, Leucanthemum vulgare, Lotus corniculatus* and *Centaurea jacea.* These species reveal the mesophile and mesothophic nature of the pastures.

Towards the upper part of the tailing dump, where the nutritional elements are fewer, the *Agrostis capillaris* and *Festuca rubra* phytocenoses begin to develop. These phytocenoses expand more and more on the tailing dumps, until they cover their middle and upper part (Table 1, column 3a).

The economic non-use of these herbal phytocenoses will facilitate the development of *Prunus spinosa* and *Crataegus monogyna* arbuscular populations coming from the edge of the forest on the tailing dumps. The development of arbuscular phytocenoses on these tailings represents a final stage in the succession of the herbal vegetation and precedes the development of the forest (Table 1, column 5).

The *Tussilago farfara* pioneer communities developed on the tailing dumps in Aghireş, due to the clayey-sandy substrata, presenting an alkaline or neutral reaction, are followed first by *Elymus repens* xero-mezophile phytocenoses. The structure of these phytocenoses, together with some xerophile species such as: *Elymus hispidus, Euphorbia cyparissias, Centaurea micranthos, Agrimonia eupatoria, Fragaria viridis* includes also some mezophile species such as: *Achillea millefolium, Cynosurus cristatus, Holcus lanatus, Medicago lupulina, Leucanthemum vulgare* and *Prunella vulgaris* (Table 1, column 2b).

Table 1. The floristic structure of the nodal vegetal communities developed on the tailing dumps in Căpuş and Aghireş.

Location of the tailing dump	**Căpuş (a)**				**Aghireş (b)**			
The vegetation phase	1	2a	3a	4a	2b	3b	4b	5
Number of phytocenological surveys	17	6	15	8	5	8	18	7
Tussilago farfara	V	III	III	.	.	I	IV	III
Poa compressa	IV	.	I	.	II	I	.	.
Calamagrostis epigejos	I	V	I	.	III	.	I	I
Agrostis capillaris	I	IV	V	V	.	II	V	I
Festuca rubra	I	.	V	I	.	V	.	I
Arrhenatherum elatius	.	.	.	V	.	I	.	III
Elymus repens	I	.	I	.	V	.	I	I
Convolvulus arvense	.	.	.	.	II	.	.	II
Galium verum	.	I	I	III	I	III	I	II
Festuca rupicola	.	.	.	.	.	.	V	.
Crataegus monogyna	.	II	.	.	I	.	II	V
Prunus spinosa	.	I	.	.	I	.	I	V
Achillea millefolium	I	III	III	II	III	III	IV	.
Achillea setacea	.	I	.	.	II	II	.	.
Agrimonia eupatoria	I	IV	III	III	III	II	IV	V
Agrostis stolonifera	II	IV	I	.	V	II	I	II

Table 1 (continued)

Location of the tailing dump	**Căpuş (a)**				**Aghireş (b)**			
Anthoxanthum odoratum	.	I	I	I	.	.	I	V
Astragalus glycyphyllos	.	.	.	I	.	.	I	I
Brachypodium sylvaticum	.	.	.	.	.	.	.	III
Campanula patula	.	.	I	I	.	.	I	.
Carex humilis	.	.	.	.	.	.	I	I
Centaurea jacea	.	.	I	III	II	I	I	II
Centaurea micranthos	II	I	I	III	III	III	.	II
Centaurea nigrescens	.	.	II	.	.	.	.	II
Centaurium pulchellum	I	IV	.	.	II	II	I	.
Cichorium inthybus	I	III	I	I	II	II	I	.
Cirsium arvense	I	II	I	.	.	.	III	I
Cerastium holosteoides	.	.	I	I	.	I	I	.
Conyza canadensis	I	II	I	.	III	III	.	.
The vegetation phase	1	2a	3a	4a	2b	3b	4b	5
Number of phytocenological surveys	17	6	15	8	5	8	18	7
Coronilla varia	.	.	.	I	.	I	I	II
Cornus sanguinea	.	.	.	I	I	I	.	I
Crepis biennis	.	.	I	I	II	I	I	.
Cynodon dactylon	.	.	I	.	.	I	.	.
Cynosurus cristatus	I	III	I	II	III	I	I	II
Dactylis glomerata	.	III	I	IV	.	I	I	V
Daucus carota ssp.*carota*	II	III	I	III	.	II	IV	.
Dianthus carthusianorum	.	.	.	III	.	I	.	.
Echium vulgare	.	.	.	III	.	.	.	.
Elymus repens	I	.	I	.	V	.	I	I
Euphorbia cyparissias	.	.	I	I	II	I	.	.
Fragaria viridis	I	IV	I	I	II	I	I	II
Galium mollugo	I	.	I	III	II	I	I	II
Geranium pratense	.	.	.	II	.	.	.	I
Hieracium pilosella	II	III	II	.	II	I	IV	.
Holcus lanatus	I	III	I	.	IV	I	III	.
Hypericum elegans	.	.	.	III	.	.	.	I

Table 1 (continued)

Location of the tailing dump	**Căpuş (a)**				**Aghireş (b)**			
Hypericum perforatum	.	II	I	II	II	I	III	.
Inula saalicina	.	.	.	.	.	.	I	.
Leontodon autumnalis	I	IV	III	I	II	III	IV	.
Leontodon hispidus	.	.	I	I	.	II	II	.
Leucanthemum vulgare	I	.	I	II	II	II	I	.
Lolium perene	.	.	I	I	.	I	I	.
Lotus corniculatus	.	.	II	IV	II	II	IV	II
Medicago falcata	.	.	.	IV	I	I	.	II
Medicago lupulina	.	.	I	I	II	II	I	.
Petrorhagia prolifera	.	.	.	II	.	I	I	.
Phleum pretense	.	.	.	III	I	II	.	III
Plantago lanceolata	I	V	III	I	III	III	II	III
Plantago media	I	III	.	III	.	I	I	I
The vegetation phase	1	2a	3a	4a	2b	3b	4b	5
Number of phytocenological surveys	17	6	15	8	5	8	18	7
Poa pratensis	.	.	I	I	.	II	I	II
Polygonum persicaria	I	II	I	.	II	I	.	.
Prunella vulgaris	.	III	I	.	II	II	II	III
Pyrus pyraster	.	I	II	I	I	.	.	.
Ranunculus acris	.	I	I	I	.	.	I	IV
Ranunculus repens	I	III	.	I	III	.	.	I
Rosa canina	.	II	.	.	.	.	II	IV
Rubus caesius	.	III	.	.	.	.	III	I
Rumex acetosella	III	.	I	.	II	.	I	.
Trifolium arvense	.	.	.	.	II	I	III	.
Trifolium campestre	.	.	.	III	.	I	I	II
Trifolium pratense	.	I	II	III	III	I	IV	.
Trifolium repens	II	III	II	.	II	I	IV	II
Taraxacum officinale	I	II	I	II	.	I	II	.
Vicia cracca	.	.	.	III	.	.	I	II
Vulpia myuros	II	III	I	.	I	I	I	.

Nodal phytocenoses in the vegetation succession on the tailing dumps

1. *Tussilago farfara* cenoses;
2a. *Calamagrostis epigejos* cenoses;
3a. *Agrostis capillaris* with *Festuca rubra* cenoses;
4a. *Arrhenatherum elatius* cenoses;
2b. *Elymus repens* cenoses;
3b. *Festuca rubra* cenoses with *Galium verum*;
4b. *Festuca rupicola* cenoses with *Agrostis capillaris*;
5. *Prunus spinosa* cenoses with *Crataegus monogyna.*

During the second succession stage, when the tailing dump begins to be structured as soil, the *Festuca rupicola* xerophile phytocenoses are mainly developed. The floristic composition of these phytocenoses includes a high prevalence of xerophile species among which: *Carex humilis, Coronilla varia, Astragalus glycyphyllos, Fragaria viridis, Galium verum, Hieracium pilosella, Inula germanica, I. salicina, Leontodon hispidus, Trifolium medium, Hypericum perforatum* and *Dianthus carthusianorum* (Table 1, column 4b). Together with these xerophile phytocenoses, in Aghireş there are also small areas of *Festuca rubra* mezophile phytocenoses with *Galium verum* and *Festuca rubra* with *Agrostis capillaris*. These are found mainly on the less steep slopes and on the small plateaus of the tailing dumps (Table 1, column 3b).

The floristic structure of these herbal phytocenoses rarely includes several arbuscular species, such as: *Crataegus monogyna, Rosa canina, Prunus spinosa* and *Ligustrum vulgare.* These will continuously develop and will form compact phytocenoses which will replace the herbal phytocenoses on the tailing dumps.

The final phase of the herbal phytocenoses is also represented in Aghireş by the *Prunus spinosa* and *Crataegus monogyna* phytocenoses (Table 1, column 5).

Conclusions

1. The vegetation of the tailing dumps is a long-term process and it is influenced by the physico-chemical properties of the tailings.

2. The first phytocenoses developed on the tailing dumps, regardless of the chemical nature of the substrata, are those developed by *Tussilago farfara.*

3. While the tailing dump begins to form as "technogenous soil" and it accommodates more and more Poacee species, the *Calamagrostis epigejos, Elymus repens, Festuca rubra* and *Festuca rupicola* mezophile and xero-mezophile phytocenoses begin to occur, which significantly contribute to the development of soil.

4. Finally, such herbal phytocenoses are replaced by *Crataegus monogyna* and *Prunus spinosa* arbuscular phytocenoses, which facilitate the development of forest phytocenoses.

REFERENCES

Anghel, G., Răvăruţ M., Turcu, G. (1971) *Geobotanica.* Ed. Ceres, Bucureşti

Cristea V., Gafta D., Pedrotti F. (2004) *Fitocenologie.* Ed. Presa Universitară Clujeană, Cluj-Napoca.

Despu I., Crişan I., Ranca P., Sălceriu V., Aramă V. (1987) *Posibilităţi de valorificare a fierului din depozitul de steril – Căpuş.* Of. Jud. pt. Stud. Ped. şi Agrochim. Cluj, mscr.: 36 pp.

Pop G. (2001) *Depresiunea Transilvaniei.* Ed. Presa Universitară Clujeană, Cluj-Napoca.

Pop G. (2007) *Judeţul Cluj,* Ed. Acad. Române, Bucureşti.

STUDIA UBB BIOLOGIA, LVII, 2, 2012 (p. 15-34)

THE EFFECT OF VARIOUS LIGHT INTENSITIES ON PHOTOSYSTEM II PHOTOCHEMISTRY IN THE CYANOBACTERIUM *SYNECHOCYSTIS* sp. PCC 6803

BOGDAN DRUGĂ[1], VICTOR BERCEA[1] and COSMIN SICORA[1,2]

SUMMARY: The cyanobacterium *Synechocystis* sp. PCC 6803 grown on BG 11 medium under air bubbling was exposed to high light intensities of 2000, 3000 and 4500 μmol.m^{-2}.s^{-1} while being in the exponential growth phase. The effect of light treatment was assessed after 15, 30, 45, 60, 75, 90, 105 and 120 minutes by monitoring chlorophyll fluorescence. F_0, F_m, Fv/Fm and Y(II) have significantly decreased under high light. The enhancement of the quantum yield of non-regular energy dissipation Y(NO) indicates that both the conversion of photochemical energy and the protective regulating mechanisms are inefficient. The increase of Y(NO) certifies the intensification of dissipation processes which take place mainly in the light harvesting antenna, in phycobilisomes. The high light intensities have led to the photoinhibition of the photosystem (PS) II antenna, affecting the reaction centers because Fv/Fm was decreased. The recovery of PSII photochemical activity was in overall a slow process correlated with light intensity that was used.

Keywords: chlorophyll fluorescence; coefficient of photochemical quenching (qP, qL); effective PS II quantum yield (Y_{II}); fluorescence yield; minimal fluorescence; maximal fluorescence; maximal PS II quantum yield (Fv/Fm); quantum yield of non-regulated energy dissipation (YNO); recovery.

[1] *Institute of Biological Research, 48 Republicii Street, 400015/Cluj-Napoca, România.*

[2, ✉] ***Corresponding author: Cosmin Sicora**, Biological Research Center, Parcului Street, no. 14, 455200/Jibou, Sălaj County, România. E-mail: cosmin.sicora@gmail.com*

Introduction

The variability of the excitation spectrum in cyanobacteria is correlated with the adaptation mechanisms of the photosynthetic apparatus with important implications on chlorophyll fluorescence. The photosynthetic apparatus adaptation to various environmental conditions such as light and nutrients (Bryant,1995; Dau, 1994; Demarsac and Houmard,1993; Müller *et al.,*1993*;* Reuter and Müller,1993) has consequences in changing the phycobilisomes content and the PS I/PS II ratio.

The chlorophyll associated to PS II has a different fluorescence production from PS I (Pfündel, 1998). The chlorophyll amount associated with photosystems is dependent on species, while its variability is induced under stress (Boekema *et al.*, 2001; Falkowski and Raven, 1997; Riethman and Sherman, 1988; Straus, 1994).

The short-time variations of the coupling energy between phycobilisomes and the two photosystems, the so-called transition-states, are associated with the redox state of the electron transport chain. By modulating the energy transport between PS I and PS II (Biggins and Bruce, 1989; Campbell *et al.,* 1998; van Thor *et al.,* 1998; Williams and Allen, 1987) it was defined the chromatic adaptation which is genetically controlled being a phenotypic response to light spectrum. The ratio between phycobilins is changing in relation to the light and its quality (Dubinsky and Stambler, 2009), while the redox state of the photosynthetic components plays an essential role (Campbell and Öquist,1996; Mullineaux and Emlyn-Jones, 2004). This variability of the photosynthetic apparatus is the consequence of an adaptation mechanism, mainly in the peripheral antenna made mostly by phycobilisomes (Bennett and Bogorad, 1973).

The studies accomplished on *Synechococcus* sp. PCC 6803 were focused on the energy transfer from phycobilisomes to photosystems (Krumova *et al.,* 2010; Ma *et al.,* 2008), on the mechanisms for lowering the fluorescence (Bissati *et al.,* 2000), and a protective mechanism of the photosynthetic apparatus in cyanobacteria due to carotenoids was emphasized (Rakhimberdieva *et al.,* 2007; 2007; 2010).

In the present study there are presented the results of monitoring the chlorophyll fluorescence in *Synechocystis* sp. PCC 6803 under various light intensities during long periods of time.

Material and methods

The cyanobacterium *Synechocystis* sp. PCC 6803 was grown at room temperature on BG 11 growth medium, under air bubbling and a moderate light intensity of 28 μmol $m^{-2}s^{-1}$ for 9 days. The cells in exponential growth phase were exposed at high light intensities of 2000, 3000 and 4500 μmol $m^{-2}s^{-1}$. The light source was an FHI-5000 W fluorescent bulb, while the light intensity was measured with a Quantum Sensor QSPAR Hansatech device. The light-treatment effect was assessed after 15, 30, 45, 60, 75, 90, 105 and 120 minutes. The 120 minutes recovery period since stopping the light treatment was monitored based on fluorescence, which was measured with a Walz Dual–100 fluorometer. The assimilatory pigments (chlorophyll a, carotenoids) were extracted with acetone and they were spectrophotometrically estimated based on specific absorption coefficients (Arnon, 1949; Lichtenthaler and Wellburn,1983), and their identification was assessed based on the absorption peak with a Jasco V-630 spectrophotometer. The phycobiliproteins were estimated based on Gantt and Lipschultz (Gantt and Lipschulz, 1974). The results are displayed in mg per liter on cell suspension.

Results and discussions

The *Synechocystis* sp. PCC 6803 culture has reached an optical density OD_{680} = 1.567. The *in vivo* absorption spectrum has displayed the spectral absorption areas of the photosynthetic apparatus components and the main absorption peaks (fig. 1). Carotenoids (481 nm) and chlorophyll a (441 nm) absorb in the blue spectral area, while phycobilins (628 nm) and chlorophyll a (682 nm) have an absorption peak in the red light.

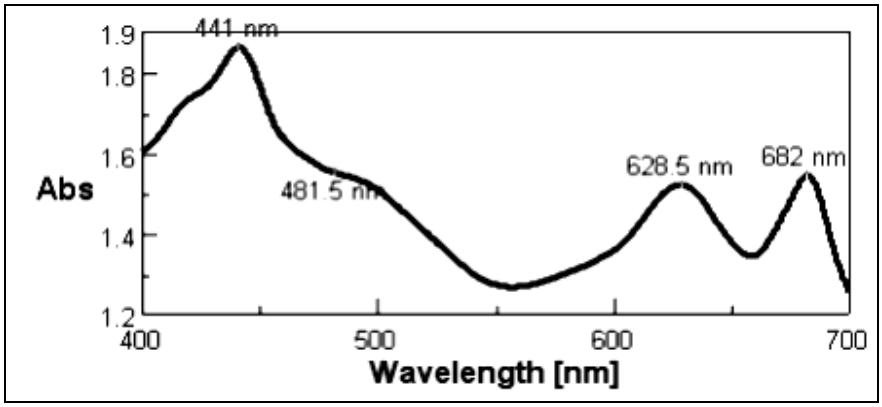

Fig. 1. *In vivo* absorption spectrum in *Synechocystis* sp. PCC 6803 grown under standard conditions.

The phycobilins are the main pigments of the light-harvesting antenna, while chlorophyll acts in photosystems reaction centers. Through photo-acclimatization the pigments amount is adjusted as an answer to light intensity (Dubinsky and Stambler, 2009). The content of assimilatory pigments which have been identified is displayed in Table 1. The components of the photosynthetic apparatus in cyanobacteria contain chlorophyll a (665 nm) which together with various carotenoids and phycobiliproteins forms the light-harvesting unit. The pigments concentration was measured right before applying the light treatment (control).

Table 1. The amount of assimilatory pigments in *Synechocystis* sp. PCC 6803 grown under standard conditions (mg/l)

Chlorophyll a	Carotenoids	Phycobiliproteins		
		Phycocyanin	Allophycocyanin	C-phycoerythrin
6.978	2.052	16.382	4.953	0.335

According to Rakhimberdieva *et al*. (2004), the major carotenoids in *Synechocystis* are zeaxanthin, β-carotene, echinenone and myxoxatnhophyll which help to energy dissipation through phycobilisomes. The carotenoids play an important role in deactivating the antenna chlorophylls under excess excitation. The protective function of carotenoids is a consequence of their short distance to chlorophylls.

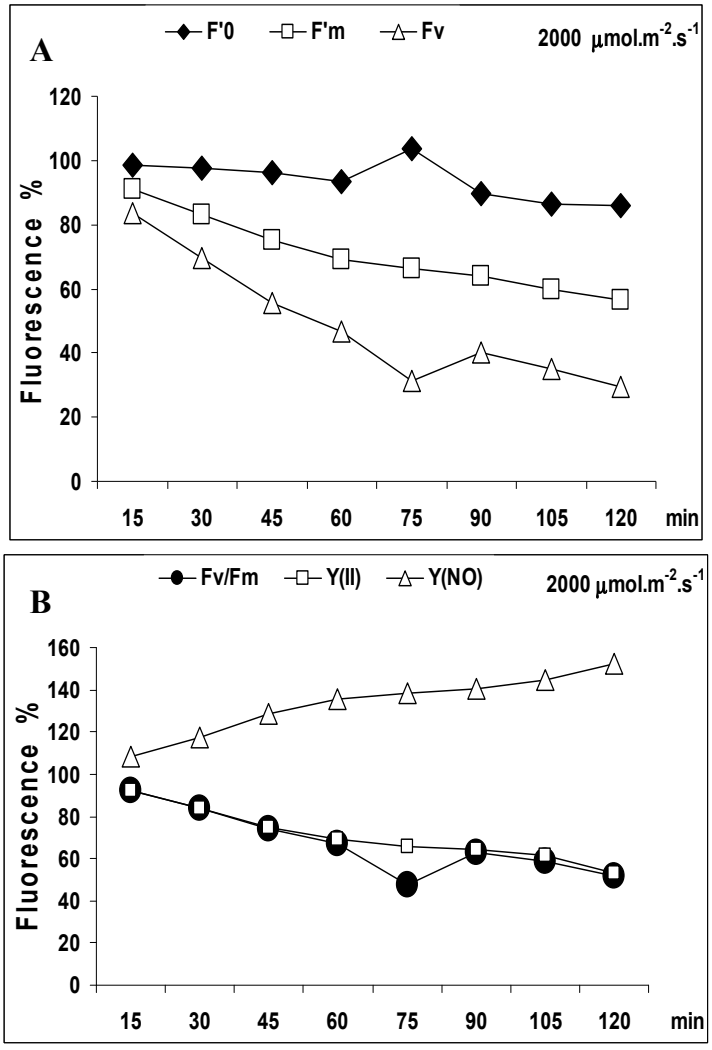

Fig. 2. Evolution of the chlorophyll a fluorescence parameters (A) and the quantum yield (B) in *Synechocystis* sp. PCC 6803 under 2000 µmol.m^{-2}.s^{-1} light intensity.

By exposing the strain *Synechocystis* sp. PCC 6803 to 2000 μmol.m^{-2}.s^{-1} light intensity, the F_0 minimum fluorescence has decreased, excepting the 75 minutes measurement. The decreasing rate at the end of the experiment was 85.82% of the control. The fluorescence main level shows that the Q_A acceptors are highly oxidized, while the PSII centers are open. The F_m a maximum fluorescence has decreased together with treatment duration to 56.52% at the experiment end (fig. 2 A). The fluorescence maximum level shows that Q_A are highly reduced, and the PSII centers are closed. The diminishing of the maximum fluorescence has led to some low values of the variable fluorescence (Fv).

The maximal quantum yield of PSII, F_v/F_m, has significantly decreased by exposing the cyanobacterial suspensions at 2000 μmol.m^{-2}.s^{-1} light intensity, generating a rate of final decrease of 51.74% (fig. 2 B). The maximum efficiency shows that light absorbed through PSII is used for reducing Q_A. The quantum yield of non-regulated energy dissipation Y(NO) has displayed an increase of 152.17%. The effective quantum yield of PSII, Y(II), has proportionally decreased together with light-exposure, showing a decrease rate of 53.44% at the end of the experiment.

The excitation energy regulation induced between the two photosystems is dependent to the moving of phycobilisomes on the thylakoid membrane and which defines the transition state. Two different mechanisms are involved in the state transition induced by light and redox state. The transition state involves the physical movement of phycobilisomes, while the redox transition involves the phycobilisomes movement and the scattering of energy between photosystems (Li *et al.,* 2004).

The photochemical quenching coefficients, qP and qL, have displayed mainly low values when compared to control (fig. 3).

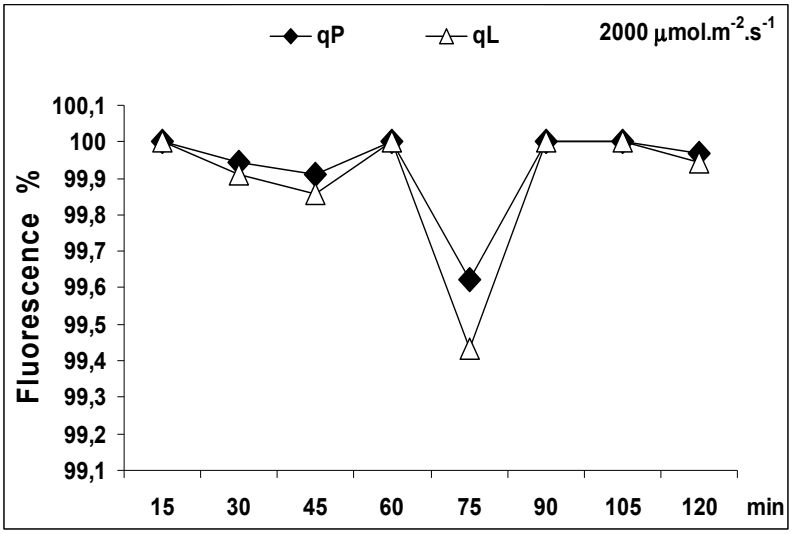

Fig. 3. Evolution of the photochemical coefficients (qP, qL) in *Synechocystis* sp. PCC 6803 under 2000 µmol.m^{-2}.s^{-1} light.

The kinetics of chlorophyll fluorescence induction shows through the analysis of the saturation pulse the evolution of each fluorescence parameter, the duration of oxidation/reduction of the Q_A primary electron acceptor and also the half time of the fluorescence curve ($T_{1/2}$), which represents the functional size of the antenna. A slow and persistent reduction of the Q_A primary electron acceptor has occurred, and also a longer period was achieved, certifying a bigger antenna for the control, while in the probe exposed to light the processes were much faster: the maximum fluorescence has decreased, while the F_m maximum fluorescence was enhanced after illumination (fig. 4).

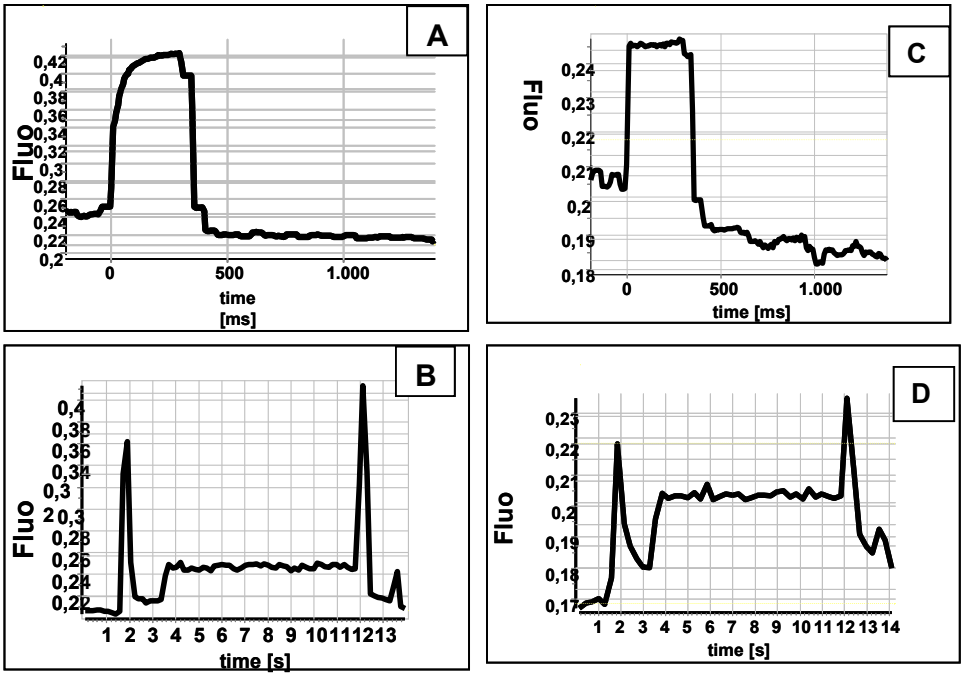

Fig. 4. The kinetics of chlorophyll fluorescence in *Synechocystis* sp. PCC 6803, control and the variant exposed to 2000 μmol.m^{-2}.s^{-1} light intensity, using the saturation pulse method: A – the kinetics of the fluorescence in control sample; B – the induction of fluorescence curve in control; C - the fluorescence kinetics under 2000 μmol.m^{-2}.s^{-1} light intensity; D – the fluorescence induction curve at 2000 μmol.m^{-2}.s^{-1} light intensity**.**

The effect of the 3000 μmol.m^{-2}.s^{-1} light intensity on the photochemical activity of PSII is presented in figure 5. The F_0 minimum fluorescence has decreased proportionally to the light exposure period, with 84.21% decrease from the control.

The F_m maximum fluorescence has significantly decreased with 57.74% at the end of the exposure period. These values have led to the diminishing of the variable fluorescence (Fv) (fig. 5 A). The maximal quantum yield of PSII has progressively decreased during light exposure, with a 57.35%

decrease at the end of the experiment (fig. 5 B). The quantum yield of non-regulated energy dissipation Y(NO) has increased with 146.10%. The effective quantum yield of PSII has decreased proportionally with the exposure period, down to 60.05% at the end of the exposure.

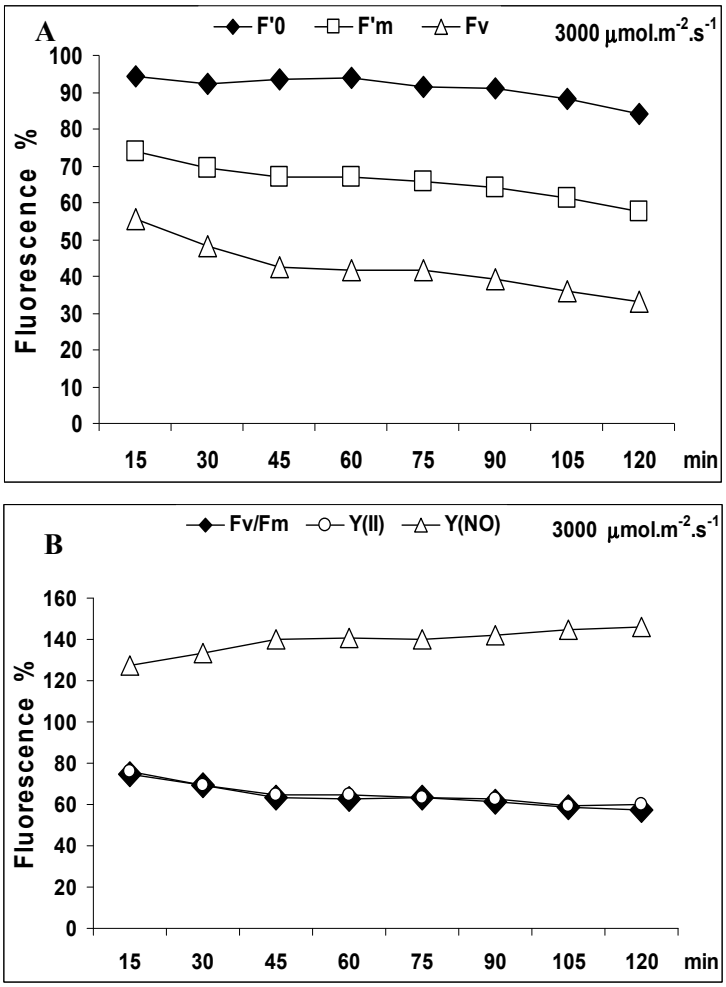

Fig. 5. Evolution of the chlorophyll fluorescence parameters (A) and the quantum yield (B) in *Synechocystis* sp. PCC 6803 under 3000 µmol.m^{-2}.s^{-1} light intensity.

The qP and qL photochemical quenching coefficients have displayed variable values under 3000 μmol.m^{-2}.s^{-1} light (fig. 6). The oxidation state of the Q_A primary electron acceptor reflects the difference in the PSII photochemical capacity and also the proportion of the oscillating "openings" during light exposure.

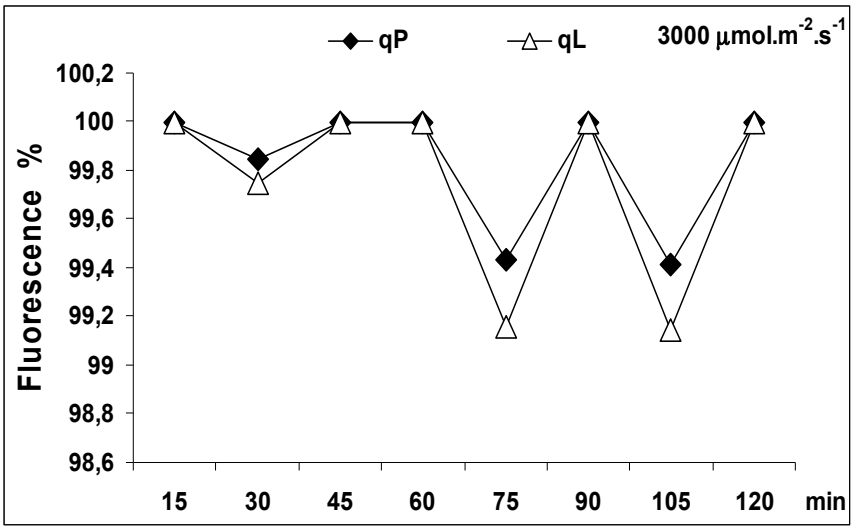

Fig. 6. The evolution of the photochemical coefficients (qP, qL) in *Synechocystis* sp. PCC 6803 under 3000 μmol.m^{-2}.s^{-1} light intensity.

The graph of the chlorophyll fluorescence kinetics through the analysis of the saturation pulse shows that a slower and longer reduction of the Q_A primary electron acceptor has occurred and a longer half time was obtaining, certifying a bigger antenna (fig. 7).

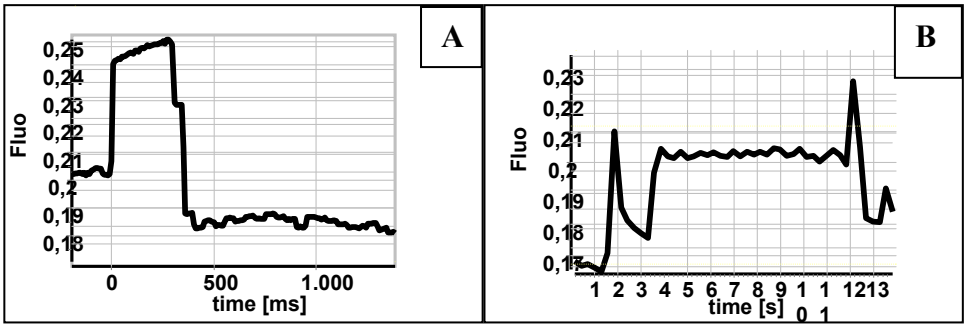

Fig. 7. The kinetics of the chlorophyll fluorescence in *Synechocystis* sp. PCC 6803 under 3000 μmol.m^{-2}.s^{-1} light intensity, using the saturation pulse method: A – fluorescence kinetics; B – fluorescence induction curve.

The effect of 4500 μmol.m^{-2}.s^{-1} light intensity on the PSII photochemical activity is presented in figure 8. The F_0 minimum fluorescence has gradually decreased during light exposure, with an 81.04% decrease at the end of the test. The F_m maximum fluorescence has significantly decreased down to 52.54% at the end of the light exposure. The diminishing of the maximum fluorescence has led to the considerably decrease of the variable fluorescence (Fv) (fig. 8 A).

The maximal quantum yield of PSII has proportionally decreased with 49.52% during light exposure (fig. 8 B). The quantum yield of non-regulated energy dissipation Y(NO) has increased with 154.27%. The PSII effective quantum yield (YII) has significantly decreased with 50.05% at the end of light exposure treatment.

The decrease of F_0, F_m fluorescence, and of the effective and maximal quantum yield and also the increase of the quantum yield of the non-regulated energy dissipation Y(NO) certify the inhibition produced by high light on the processes that take place in the photosystems antennas and PSII reaction centers.

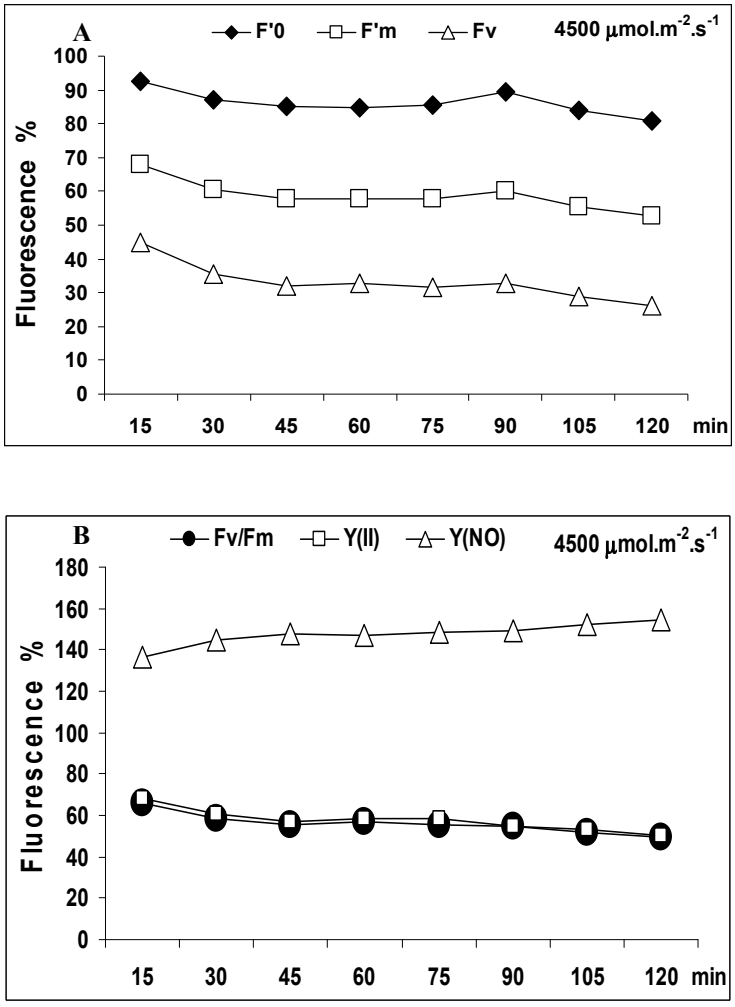

Fig. 8. The evolution of the chlorophyll fluorescence parameters (A) and the quantum yield (B) in *Synechocystis* sp. PCC 6803 4500 μmol.m^{-2}.s^{-1} light.

The photochemical quenching coefficients qP (the fraction of open reaction centers able of pohotochemistry) and qL (oxidized Q_A), have gain in generally lower values during the 4500 μmol.m^{-2}.s^{-1} light treatment (fig. 9). qP comes from using the excitation energy inside PSII in order to lead the electron transport from P_{680} to Q_A. "Open" refers to the PSII reaction center where the Q_A primary acceptor is oxidized and is able of photoreduction, while "closed" denotes the reaction center where Q_A is reduced and unable to photochemically perform anymore.

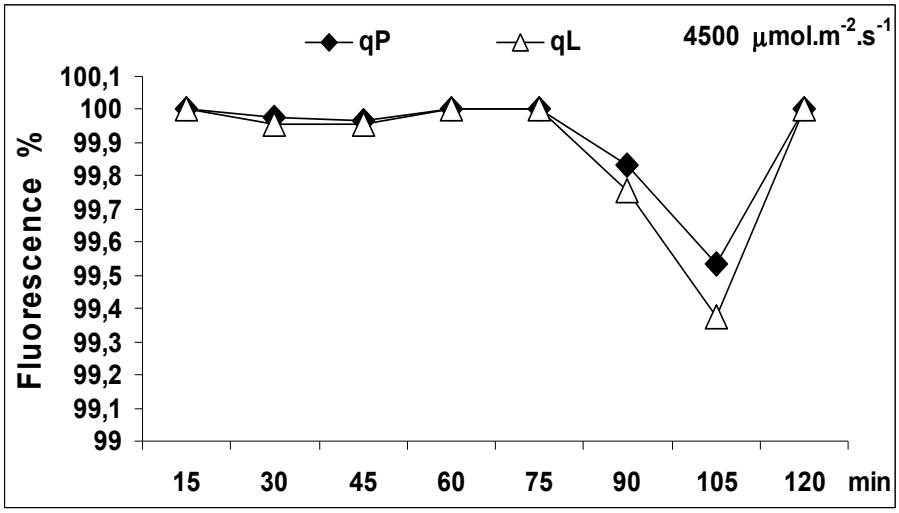

Fig. 9. The evolution of the photochemical coefficients in *Synechocystis* sp. PCC 6803 under 4500 μmol.m^{-2}.s^{-1} light.

The kinetics of chlorophyll fluorescence induction by analyzing the saturation pulse has shown that a slower but longer reduction of the primary electron acceptor Q_A has occurred, as well as a longer half-time which suggests a bigger antenna (fig. 10).

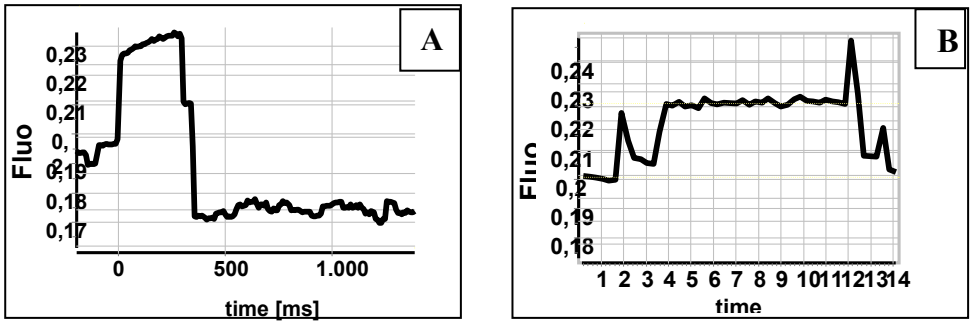

Fig. 10. The kinetics of the chlorophyll fluorescence in *Synechocystis* sp. PCC 6803 under 4500 µmol.m^{-2}.s^{-1} light intensity, using the saturation pulse method: A – fluorescence kinetics; B – fluorescence induction curve.

During the recovery period of the photosynthetic apparatus subsequent to various high light intensities the following results were achieved: F_0 value has remained higher that in control in the samples previously treated with 2000 and 3000 µmol.m^{-2}.s^{-1} light; F_m has remained low; the maximal quantum yield has remained low, while the non-regulated energy dissipation has stayed high (fig. 11).

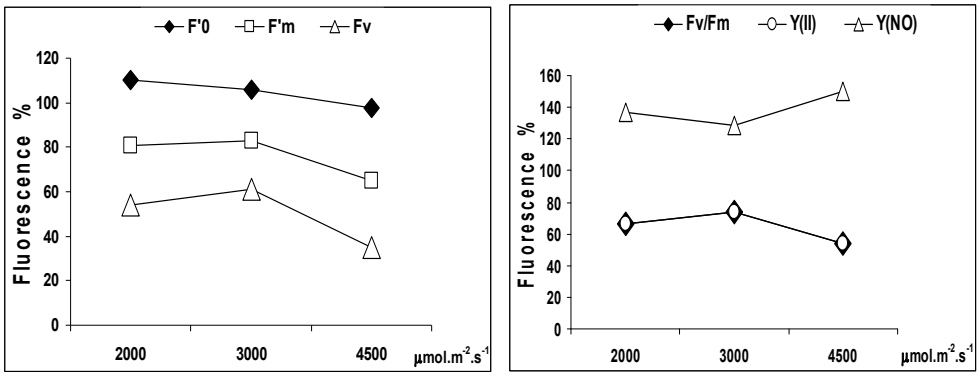

Fig. 11. The evolution of the chlorophyll fluorescence parameters in *Synechocystis* sp. PCC 6803 during the recovery period after exposure to various light intensities.

During the recovery period, the photochemical coefficients were significantly reduced (fig. 12). The cells exposed to high light have significantly reduced their photochemical quenching coefficients. The process of recovery of the PSII photochemical functionality was rather slow.

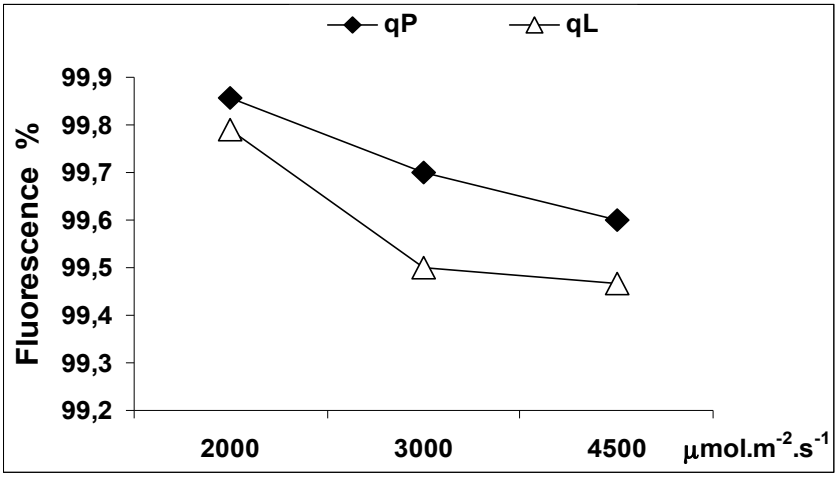

Fig. 12. The evolution of the photochemical coefficients in *Synechocystis* sp. PCC 6803 during the recovery period after exposure to various light intensities

The increase of F_0 and decrease of F_m are due to photoinhibition (van Wijk and Hasselt, 1993). Low F_m suggests the decrease of the closed Q_A number, while the interval of the excitation at the marginal receptor is shorter (Laisk *et al.,* 1997). The fluorescence emitting is influenced by the antenna heterogeneity and reduced border heterogeneity (Lazár, 1999). The dissipation of the non-radiative excitation energy in photosystems antenna leads to the F_0 and F_m decrease and the dissipation of the reaction centers reduce only the F_m (Gilmore and Yamamoto, 1991).

The PSII photoinhibition is characterized by the quantic efficiency decline, by the decrease in the number of centers involved in the linear transport of the photosynthetic electrons and by increasing the number of centers involved in the excitation energy dissipation (Critchley and Russell, 1994). Vass *et al*. (1992) have observed that and increased F_0 may be the consequence of the double reduction and of the putative protonation of Q_A, or is it is due to the separation of the PSII reaction centers (Srivastava *et al.,* 1997).

The decrease of Fv/Fm due to the increase of F_0 or decrease of F_m is a conventional measure of photoinhibition as well as an indicator of the PSII photochemical efficiency reduction because the Fv/Fm ratio is strongly connected to the quantum yield of the photosynthetic O_2 evolution or CO_2 assimilation. A fast increasing of F_0 may be induced by inactivating of a part of the PSII reaction centers (Harel *et al.,* 2004). The PSII photoinactivation (photoinhibition), the recovery reaction and the interactive photoprotective mechanisms are fundamental components of metabolism, physiology and ecophysiology of oxygenic photoautotrophic organisms (Campbell and Tyystjärvi, 2012).

Conclusions

Synechocystis sp. strain PCC 6803 has displayed an increase and a composition of the assimilatory pigments specific for its species.

Under high light intensities, the chlorophyll fluorescence parameters have significantly decreased in the illuminated samples (F_0, F_m, Fv/Fm and YII). The low values certify the use of absorbed energy mainly as chemical energy through photochemical charges separation in the RC II reaction centers. The high value of the quantum yield of the non-regulated energy dissipation shows that both the photochemical energy conversion and the protective regulator mechanisms are inefficient. The increase of the quantum

yield of non-regulated energy dissipation certifies the intensity of the dissipation processes that occur mainly in the light harvesting antenna, in the phycobilisomes.

The high light intensities that were used in this study have led to photoinhibition of the PSII antenna, affecting the reaction centers because the maximal quantum yield has decreased. The efficiency of the energetic mechanisms in the antenna and reaction centers is observed with accuracy through the kinetics of chlorophyll fluorescence induction by analyzing the saturation pulse.

The recovery of the PSII photochemical activity was, in general, a slow process, in relation with the light intensity that the cell suspensions were exposed to.

Acknowledgements. This research was supported by POS-CCE Program, project no. 236/16.08.2010.

REFERENCES

Arnon, D.I. (1949) Copper enzymes in chloroplasts. Polyphenyloxidase in *Beta vulgaris*. *Plant Physiol*., **24**, 1-15.

Bennett, A., Bogorad, L. (1973) Complementary chromatic adaptation in a filamentous blue-green alga. *J. Cell Biol*., **58**, 419-435.

Biggins, J., Bruce, D. (1989) Regulation of excitation energy transfer in organisms containing phycobilins. *Photosynth. Res*., **20**, 1-34.

Bissati, K.E., Delphin, E., Murata, N., Etienne, A.L., Kirilovsky, D. (2000) Photosystem II fluorescence quenching in the cyanobacterium *Synechocystis* PCC 6803: involvement of two diferent mechanisms. *Biochim. Biophys. Acta,* **1457**, 229-242.

Boekema, E.J., Hifney, A., Yakushevska, A.E., Piotrowski, M., Keegstra, W., Berry, S., Michel, K.P., Pistorius, E.K., Kruip, J. (2001) A giant chlorophyll-protein complex induced by iron deficiency in cyanobacteria. *Nature*, **412**, 745-748.

Bryant, D.A. (1995) *The molecular biology of cyanobacteria*. Kluwer Academic Publisher, Dordrecht.

Campbell, D., Öquist, G. (1996) Predicting light acclimation in cyanobacteria from non-photochemical quenching of photosystem II fluorescence, which reflects state transitions in these organisms. *Plant Physiol*., **111**, 1293-1298.

Campbell, D., Hurry, V., Clarke, A.K., Gustafsson, P., Öquist, G. (1998) Chlorophyll fluorescence analysis of cyanobacterial photosynthesis and acclimation. *Microbiol. Mol. Biol.Rev.,* **62**, 667-683.

Campbell, D.A., Tyystjärvi, E. (2012) Parameterization of photosystem II photoinactivation and repair. *Biochim.Biophys.Acta*, **1817,** 258–265.

Critchley, C., Russell, A.W.(1994) Photoinhibition of photosynthesis in vivo: the role of protein turnover in photosystem II. *Physiol.Plant.,* **92**, 188-196.

Dau, H. (1994) Short-term adaptation of plants to changing light intensities and its relation to photosystem-II photochemistry and fluorescence emission. *J. Photochem. Photobiol.,* **26**, 3-27.

Demarsac, N.T., Houmard, J. (1993) Adaptation of cyanobacteria to environmental stimuli new steps towards molecular mechanisms. *FEMS Microbiol.Rev.,* **104**, 119-189.

Dubinsky, Z., Stambler, N. (2009) Photoacclimation processes in phytoplankton: mechanisms, consequences, and applications. *Aquat Microb Ecol.,* **56**, 163–176.

Falkowski, P.G., Raven, J.A. (1997) *Aquatic photosynthesis*. Blackwell Science, Oxford.

Gantt, E., Lipschulz, C. (1974) Phycobilisomes of *Porphyridium cruentum*: pigment analysis. *Biochemistry*, **13,** 2960-2966.

Gilmore, A.M., Yamamoto, H.Y. (1991) Zeaxanthin formation and energy-dependent fluorescence quenching in pea chloroplasts under artificially mediated linear and cyclic electron transport. *Plant Physiol.,* **96,** 635-643.

Harel, Y., Ohad, I., Kaplan, A. (2004) Activation of photosynthesis and resistance to photoinhibition in cyanobacteria within biological desert crust. *Plant Physiol*., **136**, 3070-3079.

Krumova, S.B., Laptenok, S.P., Borst, k J.W, Ughy, B., Gombos, Z., Ajlani, G.B., Amerongen H. (2010) Monitoring photosynthesis in individual cells of *Synechocystis* sp. PCC 6803 on a picosecond timescale. *Biophy.J.*, **99**, 2006–2015.

Laisk, A., Oja, V., Rasulov, B., Eichelmann, H., Sumberg, A. (1997) Quantum yields and rate constants of photochemical and non-photochemical excitation quenching. *Plant Physiol.,* **115**, 803-815.

Lazár, D. (1999) Chlorophyll a fluorescence induction. *Biochim.Biophys.Acta.,* **1412**, 1-28.

Li, D., Xie, J., Zhao, J., Xia, A., Li, D., Gong, Y. (2004) Light-induced excitation energy redistribution in *Spirulina platensis* cells: ‘‘spillover’’ or ‘‘mobile PBSs’’? *Biochim. Biophys. Acta,* **1608**, 114– 121.

Lichtenthaler, H.K., Wellburn, A.R. (1983) Determination of total carotenoids and chlorophylls a and b of leaf extracts in different solvents. *Biochem. Soc. Trans.,* **603**, 591-592.

Ma, W., Chen, L., Wei, L., Wang, Q. (2008) Excitation energy transfer between photosystems in the cyanobacterium *Synechocystis* 6803. *J. Luminescence*, **128**, 546–548.

Mullineaux, C.W., Emlyn-Jones, D. (2004) State transitions: an example of acclimation to low-light stress. *J. Exp. Bot.*, **56**, 389-393.

Müller, C., Reuter, W., Wehrmeyer, W., Dau, H., Senger, H. (1993) Adaptation of the photosynthetic apparatus of *Anacystis nidulans* to irradiance and CO2-concentration. *Bot. Acta*, **106**, 480-487.

Pfündel, E. (1998) Estimating the contribution of photosystem I to total leaf chlorophyll fluorescence. *Photosynth. Res.*, **56**, 185-195.

Rakhimberdieva, M.G., Stadnichuka, I.N., Elanskayab, I.V. Karapetyana, N.V. (2004) Carotenoid-induced quenching of the phycobilisome fluorescence in photosystem II-deficient mutant of *Synechocystis* sp. *FEBS Letters*, **574**, 85–88.

Rakhimberdieva, M.G., Bolychevtsevaa, Y.V., Elanskayab, I.V., Karapetyana, N.V. (2007) Protein–protein interactions in carotenoid triggered quenching of phycobilisome fluorescence in *Synechocystis* sp. PCC 6803. *FEBS Lett.*, **581**, 2429–2433.

Rakhimberdieva, M.G., Elanskaya, I.V., Vermaas, W.F.J., Karapetyan, N.V. (2010) Carotenoid-triggered energy dissipation in phycobilisomes of *Synechocystis* sp. PCC 6803 diverts excitation away from reaction centers of both photosystems. *Biochim. Biophys. Acta*, **1797**, 241–249.

Reuter, W., Müller, C. (1993) Adaptation of the photosynthetic apparatus of cyanobacteria to light and CO_2. *J. Photochem. Photobiol.*, **21**, 3-27.

Riethman, H.C., Sherman, .A. (1988) Purification and characterization of an iron stress induced chlorophyll-protein from the cyanobacterium *Anacystis nidulans* r_2. *Biochim. Biophys. Acta*, **935**, 141-151.

Srivastava, A., Guisse, B., Greppin, H., Strasser, R.J. (1997) Regulation of antenna structure and electron transport in Photosystem II of *Pisum sativum* under elevated temperature probed by the fast polyphasic chlorophyll *a* fluorescence transient:OKJIP. *Biochim. Biophys. Acta*, **1320,** 95-106.

Straus, N. (1994) Iron deprivation: Physiology and gene regulation. In: *The molecular biology of cyanobacteria* (ed. Bryant, D), pp. 731-750. Kluwer Academic Press, Dordrecht.

van Thor, J.J., Mullineaux, C.W., Matthijs, H.C.P., Hellingwerf, K.J. (1998) Light harvesting and state transitions in cyanobacteria. *Bot.Acta*, **111**, 430-443.

van Wijk, K.J., van Hasselt, P.R. (1993) Kinetic resolution of different recovery phases of photoinhibited photosystem II in cool-acclimated and non-acclimated spinach leaves. *Physiol.Plant.,* **87**, 187-198.

Vass, I., Styring, S., Hundal, T., Koivuniemi, A., Aro, E.M., Andersson, B.(1992. Reversible and irreversible intermediates during photoinhibition of photosystem II: stable reduced Q_A species promote chlorophyll triplet formation. *Proc. Natl. Acad. Sci. USA,* **89**, 1408-1412.

Williams, W.P., Allen, J.F. (1987) State 1/state 2 changes in higher plants and algae. *Photosynth.Res.,* **13**, 19-45.

**** Dual-PAM-100 Measuring System for Simulaneous Assessment of P700 and Chlorophyll Fluorescence. Heinz Walz GmbH, 2006.

STUDIA UBB BIOLOGIA, LVII, 2, 2012 (p. 35-52)

THE STUDY OF PHOTOSYSTEM II (PS II) ACTIVITY BASED ON CHLOROPHYLL FLUORESCENCE IN *APHANIZOMENON ELENKINII* AICB 709, UNDER LIGHT STRESS CONDITIONS

ADRIANA HEGEDŰS[1], VICTOR BERCEA[1] and COSMIN SICORA[1, 2, ✉]

SUMMARY. High light-induced changes of chlorophyll fluorescence during 2 hours are analyzed in cyanobacteria *Aphanizomenon elenkinii* AICB 709. The light of 800 μmol.m^{-2}.s^{-1} produced the increasing of F0 and Fm in the first part of light exposure. Fv and the maximal and effective quantum yields decreased after 30 min. of light exposure. The opening state and the ratio of the reaction centers decreased. The light of 1500 μmol.m^{-2}.s^{-1} induced the rising of F0, Fm and Fv and the decreasing of maximal and effective quantum yields, relative to control. The decreasing of photochemical coefficients means that the fraction of the opened reaction centers and their ratio also were significantly diminished. The light of 2100 μmol.m^{-2}.s^{-1} determined the increasing of F0 in the first 15 min, and the decreasing of Fm, Fv, quantum yields and photochemical coefficients. The quantum yield of non-regulated energy dissipation Y(NO) enhanced in every light intensity that was used. Changes in fluorescence chlorophyll are caused by structural changes in the antenna and the PS II reaction centers due to photoinhibition produced by high light. The fast recovery of the photosynthetic parameters was obtained in the samples exposed to high light intensity.

[1] *Institute of Biological Research, 48 Republicii Street, 400015/Cluj-Napoca, România.*
[2, ✉] ***Corresponding author: Cosmin Sicora.*** *Biological Research Center, Parcului Street, no.14, 455200/ Jibou, Sălaj County, România. E-mail: cosmin.sicora@gmail.com*

Keywords: carotenoid, chlorophyll a, coefficient of photochemical quenching, effective quantum yield, minimal and maximal fluorescence, maximal quantum yield, phycobilisomes, quantum yield of non-regulated energy dissipation, recovery, saturation pulse method.

Introduction

The large density of the photons flux causes damages in the photosynthetic apparatus due to the excessive absorbed energy that can not be used in photochemistry. To avoid the photo-oxidative damages, the photosynthetic microorganisms developed regulating mechanisms for the efficient conversion of the excitation energy into heat (Jahns and Miehe, 1996).

The inactivation process is named photoinhibition. The inactivation level of PS II was quantified through the determination of slow relaxing component (qI) of the fluorescence non-photochemical quenching (qN) (Krause and Weis, 1991; Quick and Stitt, 1989) and through the measuring of the changes in Fv/Fm.

Photoinhibition involves at least two inactivation stages. The first stage is considered reversible and is produced in approximately one hour without any damages of PS II (Leitsch *et al.,* 1994). The second stage is supposed to be associated with damages of the PS II reaction center. It is likely that this stage is oxygen dependent and it is reversible through the replacement of D1 protein (Aro *et al.,* 1993; Leitsch *et al.,* 1994).

Photoinhibition is a process common to plants and cyanobacteria (Krupa *et al.,* 1990; Lönneborg *et al.,* 1988; Samuelsson *et al.,*1985; 1987). The photoinhibition installs when the captured energy exceeds the dissipated energy as a result of the rising in light intensity or as a result of moderate light when an excessive harvesting antenna is present, or if the low temperature limits the dissipation of the energy (Huner *et al.,* 1993).

The most sensitive spot to photoinhibition is the reaction center of PS II through which the key reactions become inactive in the first place, *in vivo. In vitro,* photoinhibition occurs after the primary charge separation if the electron donation to the oxidized reaction center of PS II is blocked, or instead through over-reducing of the primary acceptor Q_A, on the electron accepting side of PS II (De Las Rivas *et al., 1992)*. Both types of inhibition are the result of the degradation of D1 protein (Shipton and Barber, 1991; Vass *et al.,* 1992). On the whole, the photosystem II photoinhibition is characterized by the declining in the quantum efficiency, number of reaction centers that took part to the linear photosynthetic electron transfer and the increasing in the number of centers which are involved in the dissipation of the excitation energy (Critchley and Russell, 1994). The increasing of the light intensity is excessive and may cause damages at the level of PS II reaction centers (Casper-Lindley and Björkman, 1998; Long*et al.,* 1994).

Changes in light intensity or in temperature induce an imbalance between the energy of the light absorbed through photochemistry and the energy used in metabolism. This type of energetic imbalance is pointed out by the shift of excitation pressure of PS II photosystem, which reflects the reductive relative state of the photosystem (Huner *et al.,* 1998).

The light harvesting regulation is necessary to balance the absorption and the usage of the light energy and to minimize the photo-oxidative damaging potential (Müller *et al.,* 2001). The great variety of cyanobacterial photosynthetic apparatus is the consequence of an adaptation mechanism located in the peripheral antenna formed by phycobilisomes (Bennett and Bogorad, 1973).

The results of the present study refer to the photosystem PS II activity pointed out by the chlorophyll fluorescence measurements in the cyanobacteria *Aphanizomenon elenkinii* AICB 709, exposed to different light intensities for prolonged periods of time.

Materials and methods

The cyanobacteria *Aphanizomenon elenkinii* AICB 709 (Nostocales) was cultivated at room temperature on BG 11 medium, using a medium light intensity of 26 $\mu mol.m^{-2}.s^{-1}$, in air-lift conditions. The growth period was set to 8 days. The cells found in exponential growth rate were subjected to high light intensities of 800, 1500 and 2100 $\mu mol.m^{-2}.s^{-1}$, for a two hour period. The light source was an incandescent lamp FHI-5000 W and the light intensity was measured with Quantum Sensor QSPAR Hansatech.

The effect of light exposure was measured during 15, 30, 45, 60, 75, 90, 105 and 120 min. During the recovery period, 120 min. from ceasing the light stress, specific fluorescence measurements were taken. The photosystem II activity was evaluated by chlorophyll fluorescence parameters of light exposed probes, using a Waltz Dual-100 fluorometer.

The assimilatory pigments (chlorophyll a and carotenoids) were extracted in acetone and spectrophotometrically estimated based on specific absorption coefficients (Arnon, 1949; Lichtenthaler and Wellburn, 1983), thus their identification was done based on the maximal absorption peak using a Jasco V-630 spectrophotometer. Phycobiliproteins were estimated after Gantt and Lipschultz (1974). The results were expressed in mg/l cellular suspension.

Results and discussions

The cell suspension of *Aphanizomenon elenkinii* AICB 709 showed on optical density OD_{680}=1.080. The *in vivo* absorption spectra emphasized the blue spectra where the carotenoids (483 nm) and chlorophyll a (438 nm) absorbed energy and the red spectra where the phycobilins (638 nm) and chlorophyll a (680 nm) absorbed energy (fig. 1). The pigment composition is listed in Table 1.

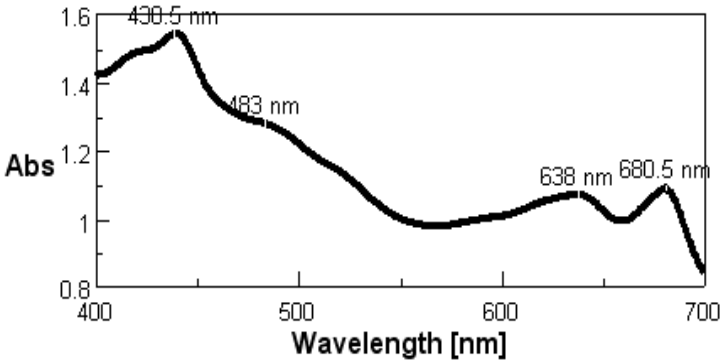

Fig. 1. *In vivo* absorption spectra of *Aphanizomenon elenkinii* AICB 709 cultures, maintained in standard growth conditions.

Table 1. The quantities of assimilatory pigments in *Aphanizomenon lenkinii* AICB 709 cultures, maintained in standard growth conditions (mg/l).

Chlorophyll a	Carotenoids	a/c	Phycobiliproteins		
			Phycocyanin	Allophycocyanin	C-phycoerythrin
5.592	1.357	4.12	4.755	6.086	4.394

In cyanobacteria, all chlorophylls are located in the antenna nucleus of PS I and PS II: the chlorophyll/P_{700} ratio is 100, and that of chlorophyll/P_{680} is 40 (Karapetyan, 2007).

Due to the exposure of *A. elenkinii* AICB 709 cells to different light intensities, the photochemical activity of the photosynthetic apparatus suffered radical changes. The effect of 800 $\mu mol.m^{-2}.s^{-1}$ resulted in a significant rising of the minimal fluorescence F_0 between 45 and 90 min. reaching a maximal increase of 178.65% at 75 min. The maximal fluorescence F_m maintained above control values for 60 min. and then decreased to 40.8% in the end. F_v decreased significantly after the first 30 min of light exposure (fig. 2 A). The maximal quantum yield Fv/Fm of PSII photosystem (photochemical efficiency) decreased to 0.35% after 30 min. in the end of the exposure, relative to control (fig. 2 B). The quantum yield of the electron transfer to

PSII (photochemistry) in the presence of light is the measure of the whole efficiency of the reaction centers and asserts the ratio of the absorbed energy by the antenna which is then used in photochemistry. The effective quantum yield $Y_{(II)}$ begun to decrease slowly after 30 min. reaching 2.6% at the end. The quantum yield of non-regulated energy dissipation Y(NO) significantly increased after 45 min. reaching a finale increase of 196.6 % to the end of the exposure. Based on the recorded values of quantum yield, after 30 min. of light exposure, some structural changes occurred in the antenna, which describe a lack of energy in the thylakoid membrane. The ratio of the opened reaction centers of PSII was high (q_P) and the non-photochemical excitation energy dissipation was insignificant. All the fluorescence parameters values emphasized the inactive state of the photosystem PSII antenna and the lowering of the photosynthetic performance. Non-radiative dissipation of the excitation energy in the photosystems antenna produced the diminishing of F_0 and F_m and the dissipation from the reaction centers reduces only Fm (Gilmore and Yamamoto, 1991). The fluorescence diminishing associated with the photoinhibition is not directly linked with the degradation of the PSII reaction centers (Briantais *et al.,* 1988).

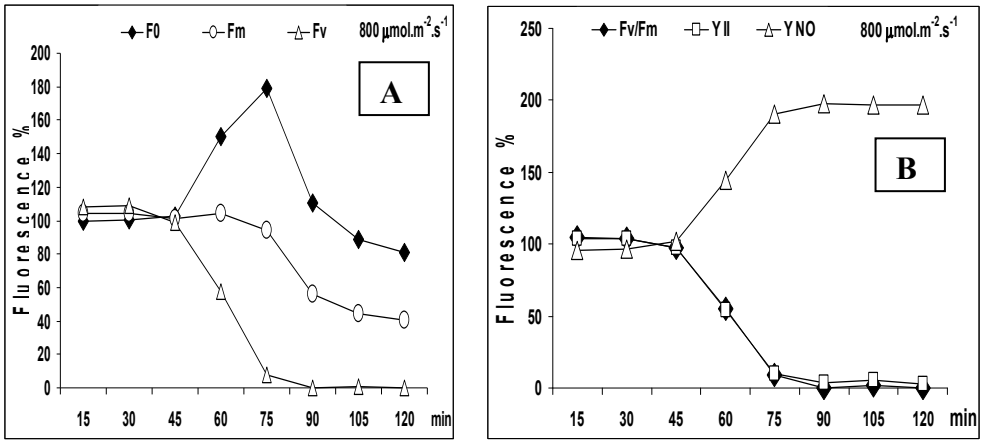

Fig. 2. The effect of 800 µmol.m^{-2}.s^{-1} light exposure on the evolution of chlorophyll fluorescence parameters (A) and the quantum yields (B) in *Aphanizomenon elenkinii* AICB 709.

On the whole, the photochemical coefficients qP and qL reached values below 1 during the entire period of high light exposure. The significant decreasing was obtained at the end of the exposure, being 87.4% relative to control. The opening level of the reaction centers and their ratio decreased relative to control due to the exposure at 800µmol.m^{-2}.s^{-1} (fig. 3). After 90 min. of light exposure, maximal values for non-photochemical energy dissipation coefficient qN was recorded. The persistence of the minimal excitation pressure (1-qP) asserts the existence of a dimensioned antenna in the context of the reduction of photosynthetic efficiency.

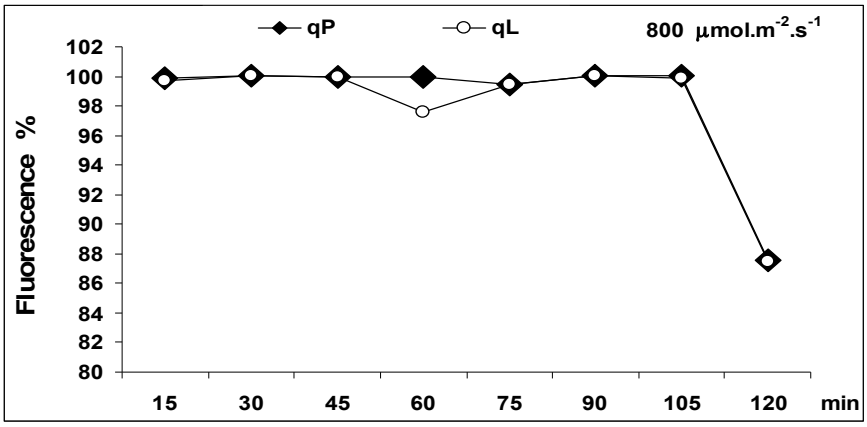

Fig. 3. The effect of 800 µmol.m^{-2}.s^{-1} light exposure on the evolution of photochemical coefficients in *Aphanizomenon elenkinii* AICB 709.

Based on the chlorophyll fluorescence induction kinetics throughout the saturation pulse the intensity of each parameter may be estimated: the duration of oxidation/reduction of the primary electron acceptor Q_A and the half time of the fluorescence curve ($T_{1/2}$) which expresses the functional size of the antenna: a rapid reduction of Q_A decreases the doubling time; a slow reduction of Q_A increases the doubling time (fig. 4).

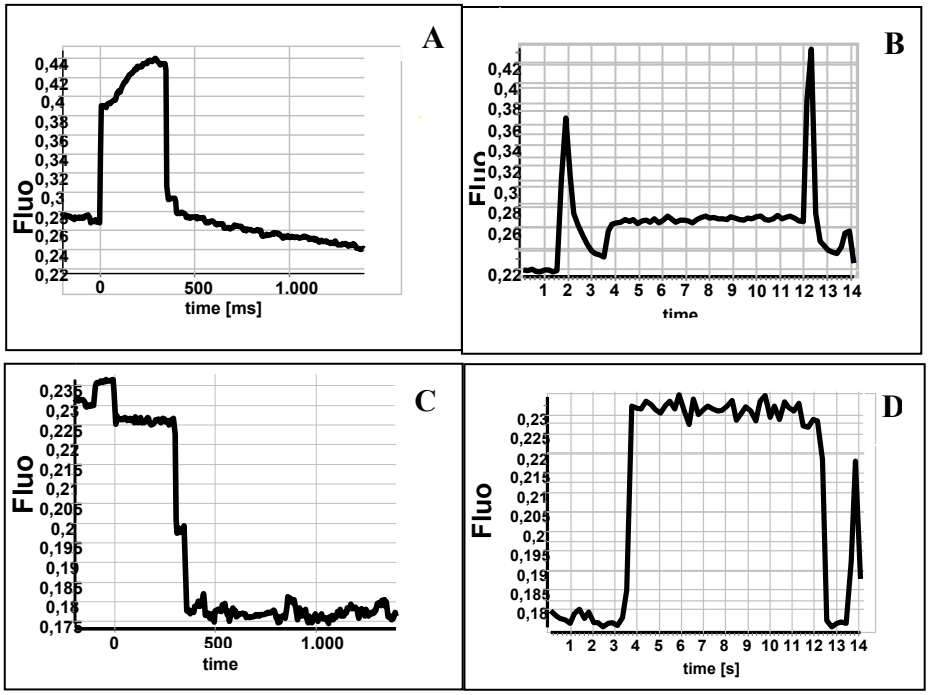

Fig. 4. The effect of high light exposure on the kinetics of chlorophyll fluorescence based on the saturation pulse method in *Aphanizomenon elenkinii* AICB 709:

A- the chlorophyll fluorescence kinetics in control;
B - the fluorescence induction curve in control;
C- the fluorescence kinetics at 800 μmol.m^{-2}.s^{-1};
D- the fluorescence induction curve at 800 μmol.m^{-2}.s^{-1}.

The light effect at 1500 μmol.m^{-2}.s^{-1} over *A. elenkinii* AICB 709 cell suspension is showed in Figure 5. F_0 increased in the first 75 min., than it decreased to 85%, relative to control. The maximal fluorescence F_m lowered proportional with the exposure time reaching 41,9% at the end, thus the closure of the reaction center is much diminished. Fv decreased significantly as a result of light exposure (fig. 5 A).

The PSII maximal quantum yield F_v/F_m decreased significantly to 0.52% at the end of the exposure and the effective quantum yield Y(II) decreased to 3% (fig. 5 B). The quantum yield of non-regulated energy dissipation, Y(NO), reached 196% at the end of the exposure.

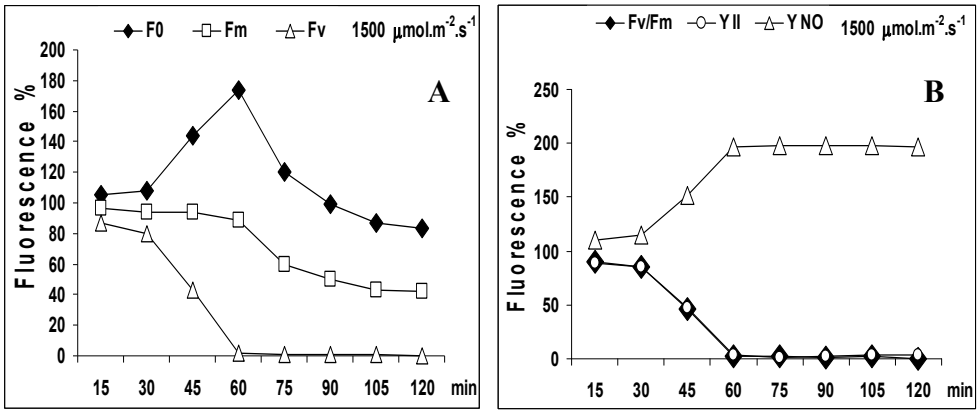

Fig. 5. The effect of 1500 µmol.m^{-2}.s^{-1} light exposure on the evolution of chlorophyll fluorescence parameters (A) and on the quantum yields (B) in *Aphanizomenon elenkinii* AICB 709.

The photochemical coefficients qP and qL significantly lowered after 45 min of exposure and they reached maximal values towards the end of the exposure when the coefficient of non-photochemical energy dissipation qN was activated. The diminishing of photochemical coefficients indicated that the ratio of the opened reaction centers and their ratio also lowered significantly (fig. 6).

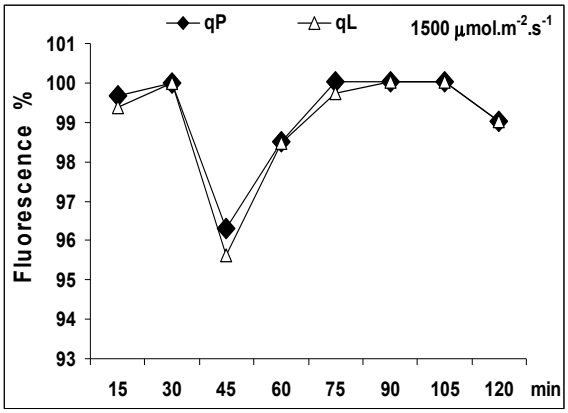

Fig. 6. The effect of 1500 µmol.m^{-2}.s^{-1} light exposure on the evolution of photochemical coefficients (qP, qL) in *Aphanizomenon elenkinii* AICB 709.

The fluorescence curve, the oxidation/reduction time of the primary electron acceptor Q_A and the half time of the fluorescence curve ($T_{1/2}$) which expresses the functional size of the antenna can be analyzed based of the chlorophyll fluorescence induction kinetics through the analysis of the saturation pulse. A quick transition of the primary electron acceptor Q_A which defines a small size antenna has occurred (fig. 7).

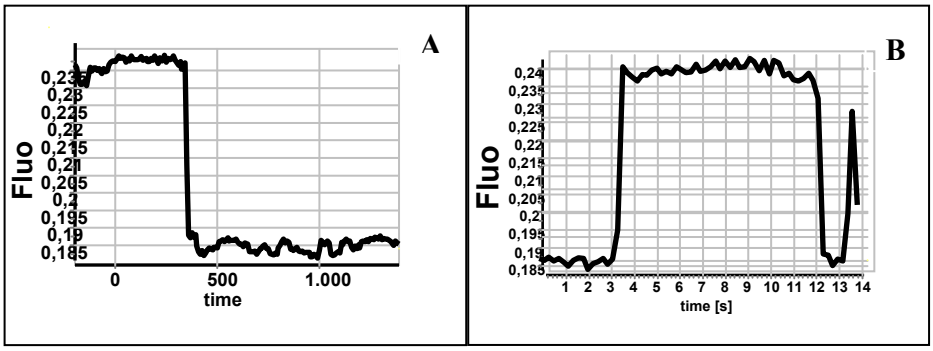

Fig. 7. The chlorophyll fluorescence kinetics using the saturation pulse method in *Aphanizomenon elenkinii* AICB 709 exposed to 1500 µmol.m^{-2}.s^{-1} light intensity. A- the chlorophyll fluorescence kinetics; B- the fluorescence induction curve.

The effect of 2100 μmol.m^{-2}.s^{-1} light intensity on PSII photochemistry is shown in Figure 8. The minimal fluorescence F_0 increased after 15 min of light exposure, reaching a maximal value of 305.9% at 45 min, thus the primary electron acceptor Q_A becomes oxidized and the reaction centers are opened, capable of photochemical performance in reducing Q_A. The maximal fluorescence F_m decreased after 60 min of light exposure leading to a finale decrease of 48.8%, relative to control. Fv decreased significantly due to light exposure (fig. 8, A).

The maximal quantum yield F_v/F_m of PS II decreased significantly to 0.29% at the end of the exposure, relative to control. The effective quantum yield $Y_{(II)}$ of PSII, decreased significantly reaching 2.2% toward the end of the exposure. The quantum yield of non-regulated energy dissipation Y(NO) increased 198.2% at the end of light exposure (fig. 8, B).

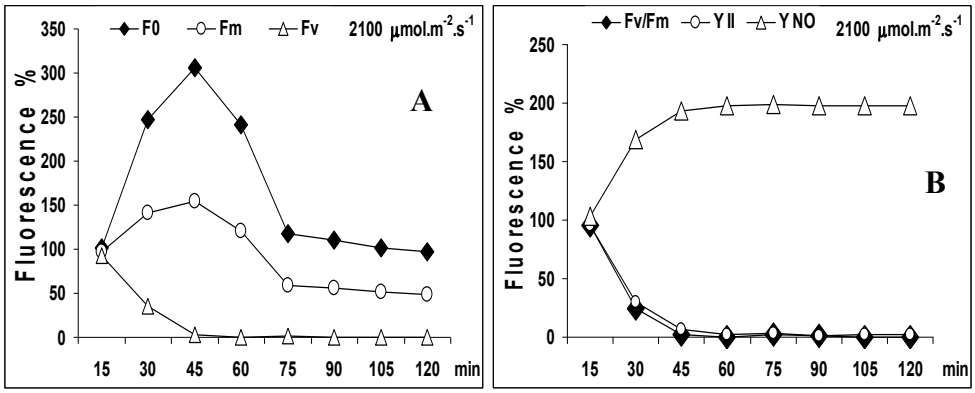

Fig. 8. The effect of 2100 μmol.m^{-2}.s^{-1} light exposure on the evolution of chlorophyll fluorescence parameters (A) and on the quantum yields (B) in *Aphanizomenon elenkinii* AICB 709.

The diminished values of photochemical efficiency F_v/F_m and the reduction of the quantum yields $Y_{(II)}$ emphasize the initiation of photosynthesis down regulation process. The mechanism of down regulation creates energy dissipation centers leading to a homogeneous down regulation through the

increasing of the quantum yield of non-regulated energy dissipation Y(NO). The mechanism of photosystems antenna is involved in dissipating the down regulation centers and the D1 turnover is important in the initiation and function of down regulation (Critchley and Russell, 1994).

The coefficients of photochemical quenching qP and qL decreased significantly at 45 and 90 min. of light exposure (fig. 9). After 45 min. of light exposure, the coefficient of non-photochemical energy dissipation qN was activated.

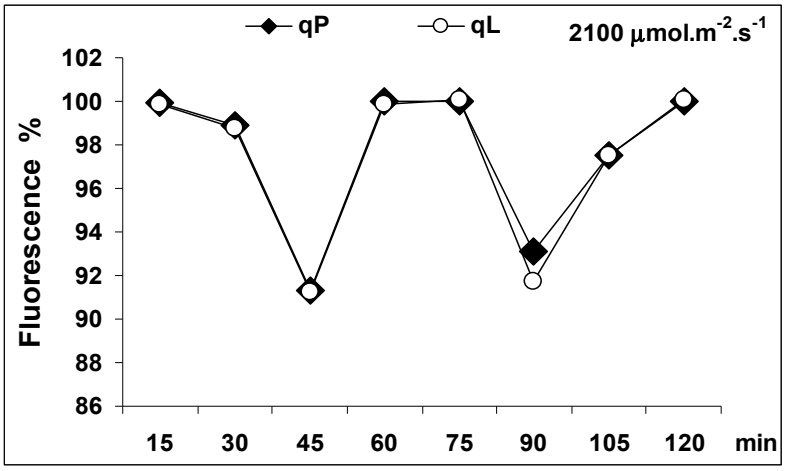

Fig. 9. The effect of 2100 µmol.m^{-2}.s^{-1} light exposure on the evolution of photochemical coefficients in *Aphanizomenon elenkinii* AICB 709.

Through the analysis of the saturation pulse, some changes in the fluorescence curve are visible, on chlorophyll fluorescence kinetics chart in the means of the oxidation/reduction period of the primary electron acceptor Q_A and in the half time of the fluorescence curve ($T_{1/2}$). A prolonged reduction of the primary electron acceptor Q_A has produced in a very short time, which asserts the existence of a diminished antenna (fig. 10).

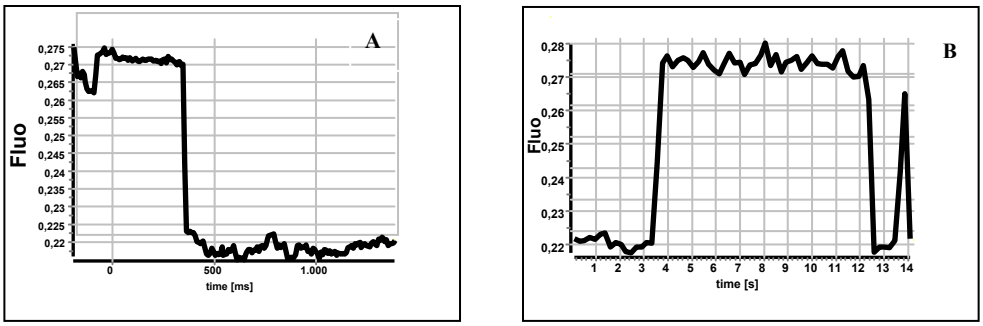

Fig. 10. The chlorophyll fluorescence kinetics using the saturation pulse method in *Aphanizomenon elenkinii* AICB 709 exposed to 2100 μmol.m^{-2}.s^{-1} light intensity. A- the chlorophyll fluorescence kinetics; B- the fluorescence induction curve.

During the recovery of the photosynthetic apparatus, the minimal fluorescence remained high relative to control (fig. 11). The maximal fluorescence increased to 67% in the case of 2100 μmol.m^{-2}.s^{-1} light exposing. The PSII maximal quantum yield and the effective quantum yield $Y_{(II)}$ remained diminished, relative to control. The quantum yield of non-regulated energy dissipation Y(NO) remained high during the recovery period, quick recoveries being recorded at 1500 and 2100 μmol.m^{-2}.s^{-1} light intensities. The photochemical coefficients reached slightly diminished values relative to control. On the whole, a more rapid recovery was observed in the cyanobacterial cell suspensions exposed to 2100 μmol.m^{-2}.s^{-1} and 1500 μmol.m^{-2}.s^{-1} respectively.

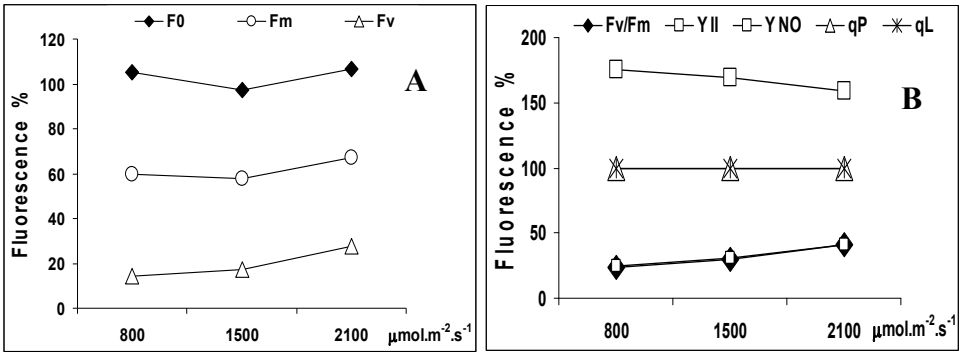

Fig. 11. The effect of various light exposures on the evolution of chlorophyll fluorescence parameters (A) and on the quantum yields (B) in *Aphanizomenon elenkinii* AICB 709, in the recovery period.

Conclusions

The *Aphanizomenon elenkinii* AICB 709 strain was cultivated at room temperature on BG 11 medium, using a medium light intensity of 26 $\mu mol.m^{-2}.s^{-1}$, in air-lift conditions. The growth curve and the composition in assimilatory pigments were species-specific. The components of the photosynthetic apparatus comprise chlorophyll a which together with various types of carotenoids and phycobiliproteins forms the light harvesting antenna.

The F_0 increased between 45 and 90 min. in conditions of 800 $\mu mol.m^{-2}.s^{-1}$ light exposure. F_m increased in the first 60 min. and than decreased to 40.8% at the end. Fv significantly decreased after the first 30 min. of light exposure. The maximal quantum yield Fv/Fm decreased in the first 30 min, reaching 0.35% at the end of the exposure. The effective quantum yield $Y_{(II)}$ gradually decreased after 30 min. reaching 2.6 % at the end of light exposure. The quantum yield of non-regulated energy dissipation, Y(NO), increased significantly after 45 min. The ratio of the opened reaction centers of PS II was high and the non-photochemical dissipation of the excitation energy was negligible. The fluorescence parameters values emphasize the inactivation state of the PSII photosystem antenna and the decreasing of

the photosynthetic performances. The photochemical coefficients qP and qL decreased, thus asserting that the opening state of the reaction center and their ratio diminished also.

The F_0 increased in the first 75 min. than decreased to 83 % in conditions of 1500 $\mu mol.m^{-2}.s^{-1}$ light exposure. F_m decreased to 41.9% in the end, which certifies that the closure of the reaction centers is much diminished.

The maximal quantum yield decreased to 0.52 % at the end of the exposure and the effective quantum yield decreased to 3%. The quantum yield of non-regulated energy dissipation recorded on increasing of 196 % at the end of light exposure. The photochemical coefficients decreased, and toward the end they reached maximal values.

F_0 increased after 15 min. in conditions of 2100 $\mu mol.m^{-2}.s^{-1}$ light exposure, thus the primary acceptor Q_A become oxidized and the reaction centers are opened, capable of photochemical performance. F_m decreased after 60 min of light exposure. The maximal quantum yield F_v/F_m of PSII significantly decreased to 0.29% relative to control at the end of light exposure. The effective quantum yield $Y_{(II)}$ of PSII decreased significantly reaching 2.2 % at the end of light exposure. The quantum yield on non-regulated energy dissipation Y(NO) recorded an increasing of 198.2 % at the end of the experiment. The photochemical coefficients significantly decreased at 45 and 90 min. of light exposure.

Through the analysis of the saturation pulse, some changes in the fluorescence curve are visible on chlorophyll fluorescence kinetics chart in the means of the oxidation/reduction period of the primary electron acceptor Q_A and in the half time of the fluorescence curve ($T_{1/2}$). A prolonged reduction of the primary electron acceptor Q_A has produced in a very short time, which asserts the existence of a diminished antenna.

A faster recovery of the fluorescence parameters was observed in the cyanobacteria cell suspensions exposed to 2100 $\mu mol.m^{-2}.s^{-1}$ and 1500 $\mu mol.m^{-2}.s^{-1}$ respectively. This cyanobacteria strain proved to be very sensitive to the light intensity.

The low values of the photochemical efficiency and that of the quantum yield and the dissipation increments emphasized the initiation of the photosynthesis photoinhibition process, leading to changes in the antenna and the reaction centers, influencing the photochemistry and the fluorescence emission.

Acknowledgements. This research was supported by POS-CCE Program, project no. 236/16.08.2010.

REFERENCES

Arnon, D.I. (1949) Copper enzymes in chloroplasts. Polyphenyloxidase in *Beta vulgaris*. *Plant Physiol*., **24**, 1-15.

Aro, E.M., Virgin, I., Andersson, B. (1993) Photoinhibition of photosystem II. Inactivation, protein damage and turnover. *Biochim. Biophys. Acta*, **1143**, 113-134.

Bennett, A., Bogorad, L. (1973) Complementary chromatic adaptation in a filamentous blue-green alga. *J. Cell Biol*., **58**, 419-435.

Briantais, J.M., Cornic, G., Hodges, M. (1988) The modification of chlorophyll fluorescence of *Chlamydomonas reinhardtii* by photoinhibition and chloramphenicol addition suggests a form of photosystem II less susceptible to degradation. *FEBS Letters,* **236**, 226-230.

Casper-Lindley, C., Björkman, O. (1998) Fluorescence quenching in four unicellular algae with different light-harvesting and xanthophyll cycle pigments. *Photosynth. Res.*, **56**, 277–289.

Critchley, C., Russell, A.W. (1994) Photoinhibition of photosynthesis in vivo: The role of protein turnover in photosystem II. *Physiol. Plant*., **92**, 188-196.

De Las Rivas, J., Andersson, B., Barber, J. (1992) Two sites of primary degradation of the D_1-protein induced by acceptor or donor side photo-inhibition in photosystem II core complexes. *FEBR Lett.*, **301**, 246-252.

Gantt, E., Lipschulz, C. (1974) Phycobilisomes of *Porphyridium cruentum*: pigment analysis. *Biochemistry*, **13**, 2960-2966.

Gilmore, A.M., Yamamoto, H.Y. (1991) Zeaxanthin formation and energy-dependent fluorescence quenching in pea chloroplasts under artificially mediated linear and cyclic electron transport. *Plant Physiol.*, **96**, 635-643.

Huner, N.P.A., Öquist, G., Sarhan, F. (1998) Energy balance and acclimation to light and cold. *Trends Plant Sci.,* **3**, 224-230.

Huner, N.P.A., Öquist, G., Hurry, V.M., Krol, M., Falk, S., Griffith, M. (1993) Photosynthesis, photoinhibition and low temperature acclimation in cold tolerant plants. *Photosynth. Res.,* **37**, 19-39.

Jahns, P., Miehe, B. 1996. Kinetic correlation of recoverii from photo-inhibition and zeaxanthin epoxidation. *Planta*, **198**, 202-210.

Karapetyan, N.V. (2007) Non-photochemical quenching of fluorescence in cyanobacteria. *Biochemistry* (*Moscow*), **72**, 1127-1135.

Krause, G.H., Weis, E. (1991) Chlorophyll fluorescence and photosynthesis: the basics. *Annu. Rev. Plant Physiol. Plant Mol. Biol.*, **42**, 313-349.

Krupa, Z., Öquist, G., Gustafsson, P. (1990) Photoinhibition and recovery of photosynthesis in *psb*A gene-inactivated strains of cyanobacterium *Anacystis nidulans. Plant Physiol.*, **93**, 1-6.

Leitsch, J., Schnettger, B., Critchley, C., Krause, G.H. (1994) Two mechanisms of recovery from photoinhibition in vivo: reactivation of photosystem II related and unrelated to D_1-protein turnover. *Planta*, **194**, 15-21.

Lichtenthaler, H.K., Wellburn, A.R. (1983) Determination of total carotenoids and chlorophylls a and b of leaf extracts in different solvents. *Biochem. Soc. Trans.,* **603**, 591-592.

Long, S.P., Humphries, S., Falkowski, P.G. (1994) Photoinhibition of photo-synthesis in nature. *Annu. Rev. Plnt Physiol. Plant Mol. Biol*., **45**, 633-662.

Lönneborg, A., Kalla, S.R., Samuelsson, G., Gustafsson, P., Öquist, G. (1988) Light-regulated expression of the *psb*A transcript in the cyanobacterium *Anacystis nidulans. FEBS Lett.*, **240**, 110-114.

Müller P., Xiao-Ping L., Niyogi K. (2001) Non-Photochemical Quenching. A Response to Excess Light Energy. *Plant Physiol.*, **125**, 1558-1556.

Quick, W.P., Stitt, M. (1989) An examination of factors contributing to non-photochemical quenching of chlorophyll fluorescence in barley leaves. *Biochim. Biophys. Acta*, **977**, 287-296.

Samuelsson, G., Lönneborg, A., Gustafsson, P., Öquist, G. (1987) The susceptibility of photosynthesis to photoinhibition and the capacity of recovery in high and low light grown cyanobacteria *Anacystis nidulans. Plant Physiol.*, **83**, 438-441.

Samuelsson, G., Lönneborg, A., Rosenqvist, E., Gustafsson, P., Öquist, G. (1985) Photoinhibition and reativation of photosynthesis in the cyanobacterium *Anacystis nidulans. Plant Physiol.*, **79**, 992-995.

Shipton, C.A., Barber, J. (1991) Photoinduced degradation of the D_1 polypeptide in isolated reaction ceners of photosystem II: evidence for an autoproteolytic process triggered by the oxidizing side of the photosystem. *Proc Natl. Acad. Sci. USA.,* **88**, 6691–6695.

Vass, I., Styring, S., Hundal, T., Koivuniemi, A., Aro, E.M., Andersson, B. (1992) Reversible and irreersible intermediates during photoinhibition of photosystem II: stable reduced Q_A species promote chlrophyll triplet formation. *Proc. Natl. Acad. Sci. USA,* **89**, 1408-1412.

**** Dual-PAM-100 Measuring System for Simulaneous Assessment of P700 and Chlorophyll Fluorescence. Heinz Walz GmbH, 2006.

STUDIA UBB BIOLOGIA, LVII, 2, 2012 (p. 53-69)

AN ESTIMATION FOR LOWER BOUND OF p53 IN DNA HEALING PROCESS; A MATHEMATICAL APPROACH

ZEINAB TANOURI [1,✉] and OMID RABIEIMOTLAGH[1]

SUMMARY: The main goal here is to estimate a lower bound for the level of the p53 protein which is necessary for the DNA damage is repaired by a coeffective work of activated p53 and ATM-p. We consider a system of ODEs as the mathematical model of interactions between the proteins p53, Mdm2, and ATM-p. The model is biologically motivated and can simulate effects of proteins on the DNA damage suppression. It is shown that positive amounts of ATM-p may force the system to pass through a saddle node bifurcation which in turn indicates the lower bound for p53. We see that if the amount of p53 is less that the lower bound then the DNA damage is not suppressed. Finally we use the bifurcation equation and show that how the Hill coefficient of p53 must be controlled in order to optimize the healing process.

Keywords: p53-Mdm2 oscillatory model, ATM-p protein, Saddle node bifurcation, Center Manifold, Hill constant.

[1] *Dept. of Applied Mathematics, University of Birjand, Birjand - Iran.*
E-mail: orabieimotlagh@birjand.ac.ir; E-mail: omid.rabiei@gmail.com
***Corresponding author**, **Zeinab Tanouri**, Dept. of Applied Mathematics, University of Birjand, Birjand, Iran. E-mail: ztanouri@gmail.com*

Introduction

In the last decades, biologists have been attempting to treatment the cancer and bind developing tumors. Nowadays, we know that a protein which is called p53 has an effective role in tumor suppressing such that, its disruption is associated with approximately 50 to 55 percents of human cancers (Almong and Rotter, 1997; Bar-Or *et al.,* 1999).

By lab observations, biologists consider three major functions for p53: as it arrests the cell cycle and gets enough time to correct the DNA damage, has an indirect role in transcription of DNA corrective proteins and finally if the above methods are not effective, performs apoptosis (programmed cell death). Because some of the cellular effects of activated p53 can be irreversible, keeping p53 function under tight control in normal cells is critical. A key player in the regulation of p53 is the Mdm2 protein. Also p53 is a transcription factor of proteins which regulates Mdm2 level (Almong *et al.,* 2000; Sigal and Rotter, 2000). This interaction imposes an intercellular negative feedback loop, which probably serves to keep p53 in tight check and to rapidly terminate the p53 response once a p53-activating stress signal has been effectively deal with (Bar-Or *et al.,* 2000). In fact, once a DNA damage occurs, an intermediate protein which is called ATM is activated, which in turn activates p53 and Mdm2 by phosphorylating this proteins (Kohn and Pommier 2005; Banin *et al.*, 1998). As there is a direct correspondence between the works of p53 and its level, so it is important to realize the dynamics due to the co-effects of proteins involved in this intercellular process.

In the last decade, mathematical models with capability to predict behaviors and simulate dependence of dynamics on parameters and variables provide a significant improvement in the dynamics analysis.

There are many mathematical models simulating the reaction between interfered proteins in cell cycle and predict the effect of parameters on final behavior of these proteins (for example see McCoy *et al.,* 2003; Hinow *et al.,* 2006; Qi *et al.,* 2007; Wagner *et al.,* 2005; Ciliberto *et al.,* 2005; Yan and Zhuo, 2006 and references within).

A recent elementary mathematical model which is motivated biologically, simulates this interaction as below (Chickarmane *et al.,* 2007).

$$\begin{cases} x' = \alpha_0 + \alpha_1 \dfrac{x^n}{k_1 + x^n} - \gamma_1 xy - \gamma_2 x \\ y' = \alpha_2 + \alpha_3 \dfrac{x^4}{k_2 + x^4} - \gamma_3 y. \end{cases} \tag{1}$$

Where x(t) and y(t) are the level of p53 and Mdm2, respectively. In the first equation α_0 represents the production rate of p53 and Mdm2, in fact it is the phosphorylation rate of p53 by ATM-p, second term represents an autocatalytic process which we assume exists due to positive feedback of p53 on itself and is described with a Hill coefficient n, which is a chemical index depends on protein molecular structure, third term describes decreasing the level of p53 by Mdm2 and the fourth term represents the degradation of p53 independently of Mdm2. Likewise, in the second equation, α_2 describes a basal production level of Mdm2, and the second term represents the activation of Mdm2 by p53, described by a Hill equation with exponent 4, the last term represents the degradation of active Mdm2.

Experimental observations show that the DNA damage activates phosphorylation process of ATM which in turn switches on the p53-Mdm2 oscillatory behavior. When the damage is repaired this oscillation is switched off by ATM-p. This is in spirit of Ciliberto, Novak and Tyson (Ciliberto *et al.,* 2005) and can be found through numerical plots of (1). This is the significance of the model (Chickarmane *et al.,* 2007) which makes it biologically motivated. As ATM-p has an important role in activating of p53, ATM-p has a direct role in α_0. Thus, in the simplest form, by assuming that this effect works linearly, the first equation in (1) must be replaced by

$$x' = z + \alpha_1 \frac{x^n}{k + x^n} - \gamma_1 xy - \gamma_2 x.$$

Here $z(t)$ stands for the amounts of the ATM-p protein at time t, which holds in the following equation

$$z' = \alpha_{1s} \frac{z(\mu - z)}{k_{1s} + \mu - z} + \alpha_{2s} \frac{z}{(k_{0d} + w)(k_{2s} + z)},$$

where w simulates the DNA damage signal. The first term of the above equation, with coefficient α_{1s} and the second term, with coefficient α_{2s} show phosphorylation and dephosphorylation rates of the ATM protein, respectively. The parameter k_{1s} controls dependence of phosphorylation rate of the ATM protein to the level of ATM. Similarly, the parameters k_{2s} and k_{0d} control dependence of dephosphorylation rate of the ATM protein to the level of ATM-p and damage signal, respectively.

Finally, the DNA is repaired by the combined actions of ATM-P and p53, which is simulated as the following equation

$$w' = -\alpha_d wxz$$

where α_d is the rate of repair in dimensionless unites. Therefore the simultaneous model of reaction between levels of these proteins gathers in the following system of differential equations

$$\begin{aligned} x' &= z + \alpha_1 \frac{x^n}{k_1 + x^n} - \gamma_1 xy - \gamma_2 x \\ y' &= \alpha_2 + \alpha_3 \frac{x^4}{k_2 + x^4} - \gamma_3 y \\ w' &= -\alpha_d wxz \\ z' &= \alpha_{1s} \frac{z(\mu - z)}{k_{1s} + \mu - z} + \alpha_{2s} \frac{z}{(k_{0d} + w)(k_{2s} + z)}. \end{aligned} \tag{2}$$

As soon as damage occurs, ATM phosphorylates itself which activates the repairing process and damps the damage signal in conditions. In fact, RabieiMotlagh and Afsharnezhad specify an area in the parameter space in which ATM-p suppresses DNA damage by a co-effective work simulated in two last equations of the model (2) (Rabieimotlagh and Afsharnezhad, 2010). They suppose that

$$\Lambda = \mu(\mu + k_{1s}) - k_{1s}k_{2s},\ U = k_{1s}(\mu + k_{1s} + k_{2s}) \quad \text{and define}$$

$$\Delta = (\mu + k_{1s})\alpha_{2s} - \mu k_{0d}k_{2s}\alpha_{1s},\ \Omega = \alpha_{2s}\sqrt{U}/\left(\alpha_{1s}(U - \sqrt{U})(\sqrt{U} - k_{1s})\right) - k_{0d}.$$

They proved that change in the sign of Δ and Ω may cause a bifurcation in the behaviour of the damage signal, (see theorem 2, Rabieimotlagh and Afsharnezhad, 2010) which can biologically interpret the DNA healing process and permanent damage. Furthermore, if the sufficient conditions for the DNA healing process satisfy, except in a null set of this area, always level of ATM-p should be eventually nonzero (see cases (c),(d) and (f) of table A of Rabieimotlagh and Afsharnezhad, 2010). This means that, in order to have the cancer disease suppressed, any control on the co-effective work of ATM-p and p53 must guarantees that the amount of the ATM-p protein remains eventually nonzero.

In what follows, we consider the two first equations of the model (2) and investigate sufficient conditions that the DNA healing process is successfully accomplished. Indeed from the first equation of (2) we know that if the amount of ATM-p is eventually nonzero, then the amount of activated p53 should be also eventually nonzero. Thus we must indicate the lower bound for the amount of activated p53 for which the DNA damage is repaired eventually by co-effective work of ATM-p and p53. We see that the non zero amount of ATM-p causes a saddle-node bifurcation and the stable manifold of the saddle point divides the phase space into two distinct regions. The right hand side region provides the sufficient conditions (the lower bound for amount of p53) for the DNA healing process. Furthermore,

we obtain the bifurcation equation with respect to the amount of ATM-p, the basal production level of Mdm2 and the Hill coefficient k_1. This helps us to understand the co-effect of the ATM-p and p53 on the healing process; indeed, as soon as the amount of ATM-p remains nonzero, the bifurcation occurs. This, in turn, controls the amount of p53 such that the damage signal is eventually damped. In the last part of the paper we put a control on the amounts of ATM-p in order to optimize the damping process.

p53-Mdm2 Oscillatory Model

Let consider the oscillatory model of p53 and Mdm2 as the following system

$$\begin{cases} x' = z + x(\alpha_1 \dfrac{x^{n-1}}{k+\beta+x^n} - \gamma_1 y - \gamma_2) = 0 \\ y' = \theta + \alpha_3 \dfrac{x^4}{k+x^4} - \gamma_3 y = 0. \end{cases} \tag{3}$$

Here z, β and θ are parameters of system. Therefore we can consider this system as a perturbation with respect to the z, β and θ of the system (1). The first step is to prove the following theorem.

Theorem 1. *For $\theta = z = \beta = 0$, the system (3) has a nonhyperbolic critical point, say (x_1, y_1), which is a bifurcation point. In fact, in the $\beta = 0$ plane the system has a saddle node bifurcation and in $z = 0$ plane it has a transecritical bifurcation*

For proving theorem 1, let define unperturbed maps

$$f(x) = \frac{1}{\gamma_1}(\alpha_1 \frac{x^{n-1}}{k+x^n}) - \gamma_2 \ , \ g(x) = \frac{\alpha_3}{\gamma_3}(\frac{x^4}{k+x^4}).$$

Notice that the unperturbed system (3) (i.e. when $\theta = z = \beta = 0$) has the origin as a critical point with the linear part $\begin{pmatrix} -\gamma_2 & 0 \\ 0 & -\gamma_3 \end{pmatrix}$ thus for z, β and θ sufficiently small, the origin is a hyperbolic sink. Other steady states are obtained by $x' = 0,\ y' = 0$ which imply respectively

$$y = f(x) = \frac{1}{\gamma_1}(\alpha_1 \frac{x^{n-1}}{k + x^n}) - \gamma_2 \quad , \quad y = g(x) = \frac{\alpha_3}{\gamma_3}(\frac{x^4}{k + x^4}).$$

The points, at which the graphs of f and g meet each other, are the singularities of the unperturbed system. For study of possibility of existence of this points notice that f has a maximum in $x_0 = \sqrt[n]{k(n-1)} > 0$. As $f(0) = -\gamma_2 / \gamma_1$ and $g(0) = 0$ so if $f(x_0) < g(x_0)$ then the graph of f dose not crosses the graph of g for $x > 0$. Also if $f(x_0) > g(x_0)$ then these two graphs have two cross points for $x > 0$. Thus by considering parameter $\nu = f(x_0) - g(x_0)$ we have proved the following lemma.

Lemma 3. *In increasing the value of ν from negative values to positive ones, there is a unique value $\nu_0 \geq 0$ such that:*

1) For $\nu < \nu_0$ system (3) has no critical point for $x > 0$ and for $\nu = \nu_0$ the system (3) has one critical point (x_1, y_1) with $0 < x_1 < x_0$.

2) For $\nu > \nu_0$ the system (3) has exactly two critical points in the $x > 0$ area. Thus for $\nu = \nu_0$ a saddle node bifurcation occurs at (x_1, y_1); (see Fig. 1).

As the saddle node bifurcation may permanent with respect to small perturbations (Guckenheimer and Holmes, 1993), we show that for $|\theta|, |\beta|, |z| > 0$ sufficiently small, system (3) has this type of bifurcation; however it is not necessarily the only bifurcation which occurs. We will see latter that the system has also a trasecritical bifurcation. In the next section we apply the center manifold method and compute the bifurcation equation.

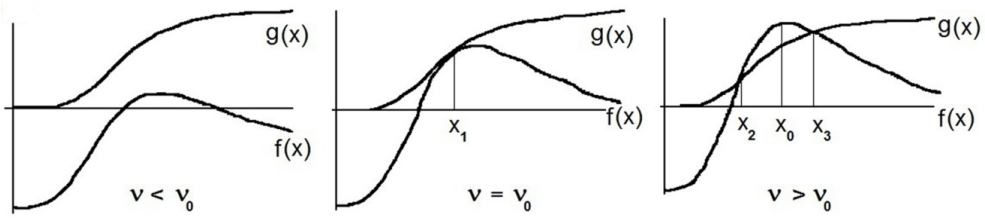

Figure 1. A saddle node bifurcation occurs for $\nu = \nu_0$ at (x_1, y_1).

Center manifold method

Let $(x_1, y_1) = (a, f(a))$, with $0 < x_1 \le x_0$, be the tangent point of the graphs (see case $\nu = \nu_0$ in (Fig. 1)). The linear part of the system at (x_1, y_1) is given by

$$\begin{pmatrix} F_x(x_1,y_1) & F_y(x_1,y_1) \\ G_x(x_1,y_1) & G_y(x_1,y_1) \end{pmatrix}$$

where $F(x,y) = \gamma_1(xf(x) - xy)$, $G(x,y) = \gamma_3(g(x) - y)$.

Since $f'(a) - g'(a) = 0$ so two eigenvalues of the system are given by $\lambda_1 = 0$ and $\lambda_2 = a\gamma_1 f'(a) - \gamma_3$. Since $f'(a) = g'(a) = (\frac{\alpha_3}{\gamma_3}) 4a^3 k / \left(k + a^4\right)^2$ so $\lambda_2 \ge 0$ if and only if $Aa^8 + (A-2)2k\, a^4 + Ak^2 \le 0$, where $A = \gamma_3^2 / \alpha_3\gamma_1$.

But $Aa^8 + (A-2)2k\, a^4 + Ak^2 = 0$ if and only if $a^4 = (k\,(2-A) \pm 2k\sqrt{1-A})/A$. This implies that $A \le 1$, but in this case $A - 2 \le 0$ and so $a^4 < 0$ which is impossible. This guarantees that $\lambda_2 = a\gamma_1 f'(a) - \gamma_3 < 0$. Thus, $(a, f(a))$ has a one dimensional center manifold and a one dimensional stable manifold. This means that the saddle node bifurcation causes two hyperbolic steady states of saddle type and sink type respectively. Furthermore the bifurcation equation is a one dimensional equation. For finding this

equation, we change the system to its standard form and calculate the associated one dimensional center manifold. Whoever, we omit the long calculations and give the results. At first, we transfer $(x_1, y_1) = (a, f(a))$ to the origin and obtain

$$\begin{cases} x' = F(x, y, z) \\ y' = G(x, y, \theta) \\ z' = 0 \\ \beta' = 0 \\ \theta' = 0 \end{cases} \qquad (4)$$

where

$$F(x,y,z) = z + \gamma_1(x+a)(f(x+a,\beta) - f(a,0) - y),$$
$$G(x,y,\theta) = \theta + \gamma_3(g(x+a) - g(a) - y),$$

with

$$f(x,\beta) = (\alpha_1 x^{n-1}/(k+\beta+x^n) - \gamma_2)/\gamma_1,$$
$$g(x) = \alpha_3 x^4/\gamma_3(k+x^4).$$

Notice that the Jordan form of the system (4) at the origin is of the form

$$J = \begin{pmatrix} \lambda_2 & 0 & 0 & 0 & 0 \\ 0 & 0 & 1 & 0 & 0 \\ 0 & 0 & 0 & 0 & 0 \\ 0 & 0 & 0 & 0 & 0 \\ 0 & 0 & 0 & 0 & 0 \end{pmatrix}.$$

Thus, the standard form of system is as the following

$$\begin{aligned} x' &= \lambda_2 x + H_1(x,y,z,\beta,\alpha_2) \\ y' &= z + H_2(x,y,z,\beta,\alpha_2) \\ z' &= 0 \\ \beta' &= 0 \\ \theta' &= 0, \end{aligned} \qquad (5)$$

where H_1 and H_2 show the nonlinear terms. Thus the center manifold equation has the local representation as below

$$x = h_2(y, z, \beta, \alpha_2) + O(3), \qquad (6)$$

where h_2 is a homogeneous polynomial of degree 2. By putting (6) in the first equation of (5), we can calculate h_2 and then putting h_2 in the second equation of (5), finally, after simplifying, the bifurcation is of the form

$$y' = z + A_0\beta^2 + A_1\beta\theta + B\beta y + Cy^2, \qquad (7)$$

where

$$0 < A_0 = \left(-a\gamma_1\gamma_3 f(a,0)\frac{\partial^2 f}{\partial \beta^2}(a,0) \right) / \lambda_2,$$

$$0 > A_1 = \left(-a\gamma_3 f(a,0)\frac{\partial f}{\partial \beta}(a,0) \right) / \lambda_2,$$

$$B = \gamma_1\gamma_3 \left(\frac{\partial f}{\partial \beta}(a,0) + a\frac{\partial^2 f}{\partial \beta^2}(a,0) \right) / \lambda_2,$$

$$C = \left\{ (a\gamma_1\gamma_3) / (\lambda_2 f(a,0)) \right\} \left(\frac{\partial^2 f}{\partial x^2}(a,0) - \frac{\partial^2 g}{\partial x^2}(a) \right).$$

Proof of theorem 2. Consider the bifurcation equation (7) with respect to the variable y=[Mdm2[t]]. The bifurcation region is determined by the sufficient condition of existence of zeroes for (7), i.e.

$$(B^2 - 4A_0C)\beta^2 - 4A_1C\theta\beta \geq 4Cz.$$

This shows that if $C < 0$ and $\beta = 0$ then crossing of $z = 0$ to the positive area of the parameters implies a saddle node bifurcation for the system (7) and so does for (3). In this case for $z, \beta > 0$ sufficiently small in the bifurcation area, the saddle node bifurcation causes two hyperbolic singularities of saddle type and sink type respectively. Also if $z = 0$ then

the bifurcation is of the form $(B^2 - 4A_0C)\beta \geq 4A_1C\theta$ which is a straight line passing through the origin. Finally, if $\theta = -A_0\beta / A_1, z = 0$ then the bifurcation equation (7) is of the form $y' = \beta y + Cy^2$ which shows a transcritical bifurcation for the system. This means that crossing the line $\theta = -A_0\beta / A_1$ in the z=0 plane causes the transecritical bifurcation in system (3)

Biological results

In the biological modeling existence of the bifurcation is important because it makes change in behavior of the system. In system (3) the level of the proteins, in particular p53, has an important role in remedy of cancer. As it is mentioned before, decline in the level of activated p53 is a certain evidence for discorrection of DNA damage. If the amount of ATM-p and the basal amount of Mdm2 are zero (i.e. $z = \theta = 0$), from the discussion after theorem 1, we know that in the absence of the saddle node bifurcation (case $\nu_0 < \nu$ in Fig. 1), the origin is the only steady state point for (3) with global attraction basin. This means that all solutions of (3) are eventually attracted by the origin (see Fig. 2).

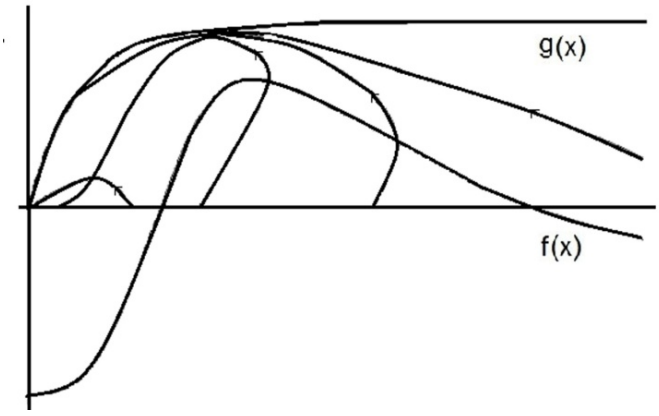

Figure 2. Attraction of solutions to the origin for $\nu < \nu_0$.
This occurs before the saddle node bifurcation.

This means biologically that the DNA damage remains permanently. As mentioned before, the necessary condition for damping the DNA damage signal in system (2) is that the amounts of the ATM-p protein should remains eventually nonzero. Thus, in order to repair the DNA damage, the positive amounts of the ATM-p (and also basal level of Mdm-2) must be controlled such that the system (3) passes through the saddle node bifurcation Indeed, the constants k_1, k_2 in the Hill formula (see the system (2)) must be enough close to each other (this guaranties that $0 \leq |\beta|$ is small enough) and the parameter values in the system (3) must be such that $\frac{\partial^2 f}{\partial x^2}(a,0) > \frac{\partial^2 g}{\partial x^2}(a)$ (this guaranties that $C < 0$).

At the bifurcation point (x_1, y_1), the stable manifold divides the phase space into two distinct regions (see Fig. 3). Due to the boundedness of solutions of (3), all solutions in the right hand side region are attracted by (x_1, y_1). Similarly, as soon as the saddle node bifurcation occurs, two singularities (x_2, y_2) and (x_3, y_3) are raised for system (3) with $x_2 < x_0 < x_3$ (see case $\nu > \nu_0$ in Fig. 1).

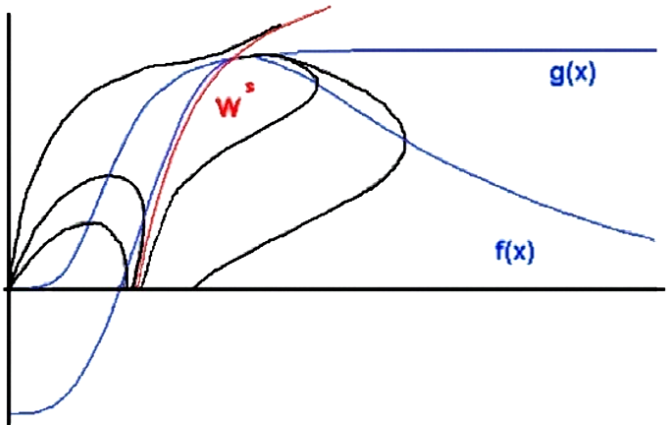

Figure 3. Behavior at the bifurcation point (x_1, y_1) for $\nu = \nu_0$.
The stable manifold W^s separates the phase space into two regions.

From the local bifurcation theory (see Guckenheimer, J., Holmes, P. 1993) we understand that x_2 is a hyperbolic saddle point and x_3 is a hyperbolic sink. In this case, the stable manifold of (x_2, y_2) divides the phase space into two distinct regions (see Fig. 4).

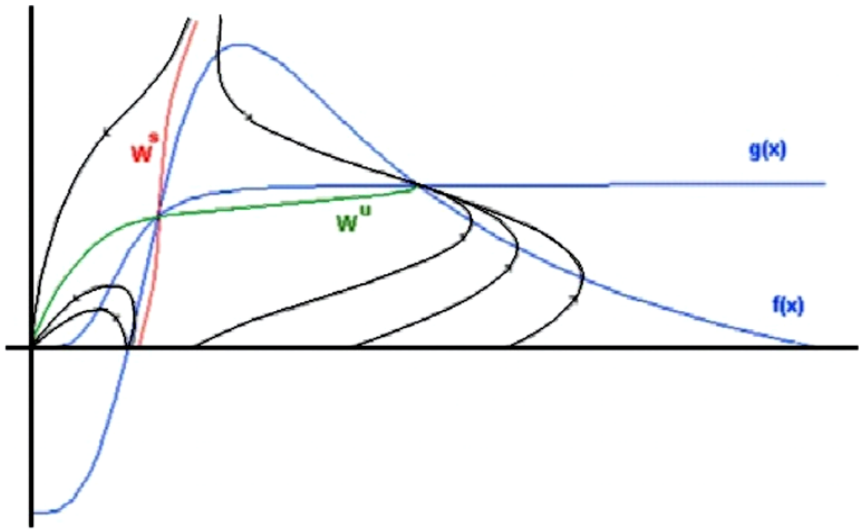

Figure 4. Behavior after the saddle node bifurcation, $\nu > \nu_0$.
Solutions in the right hand side region are attracted by (x_3, y_3)

All solutions in the right hand side region are attracted by (x_3, y_3). This means that In the right hand side region of the stable manifold, the level of activated p53 remains eventually nonzero which in turn damp the DNA damage signal with a co effective work with ATM-p; whoever in the left hand side region of the stable manifold the level of activated p53 may eventually converges to zero which is a certain evidence for discorrection of the DNA damage. Thus, as it is shown in the (Fig. 3, Fig. 4), the stable manifold indicates the lower bound of amounts of p53 (and simultaneously Mdm2) for which the DNA damage signal is eventually damped.

Optimal Control

Results of the previous section convince us that a fair optimal control on the system (3) must control positive amounts of the ATM-p such that the system (3) passes through the saddle node bifurcation. It must also push the solutions of the system to the attraction basin of the hyperbolic sink arisen from the saddle node bifurcation. For this purpose, we consider the positive amounts for $z=[ATM-p](t)$ and parameters such that the system (3) passes through the saddle node bifurcation. For simplicity, we assume that $\theta=-A_0\beta/A_1$ and consider β as the control function. Thus the bifurcation equation has the following form

$$y'=z+B\beta y+Cy^2.$$

The goal is finding the function $\beta(t)$ such that $\beta(t)$ converges approximately to zero and the solution $y(t)$ of the bifurcation system after a specific time converges to the hyperbolic sink, that is $y(0)=y_0$, $y(T)=\sqrt{-C/z}$, $\beta(T)\approx 0$. Moreover $\beta(t)$ must minimize the convergence pass by minimizing the positive function $J=\int_0^T (y-\sqrt{-C/z})^2+\beta^2 dt$. Thus the Hamiltonian function of the problem is of the form

$$H(y,\beta,\lambda)=\lambda(z+B\beta y+Cy^2)+(y-\sqrt{-C/z})^2+\beta^2.$$

Also the *Pontryagin's* minimum principle is $\partial H/\partial\beta=B\lambda y+2\beta=0$ which implies that

$$\beta=-By\lambda/2. \tag{8}$$

Finally the Euler-Lagrange equation of this problem is as the following form

$$y' = z + (C - \frac{1}{2}B^2\lambda_2)y^2 \ ,$$

$$\lambda_2' = -\lambda_2(2Cy - \frac{1}{2}B^2\lambda_2 y) - 2(y - \sqrt{-C/z}) \qquad (9)$$

where $\lambda(T) = 0$. This means that the optimal function $\beta(t)$ is found among solutions of the equations (8) and (9) simultaneously. A numerical plot for such function is shown in the Fig. 5, when the function $\beta(t)$ is drawn for $-C = B = z = 1$. Obviously the solution $y(t)$ of the bifurcation equation and the control function $\beta(t)$ converge to $\sqrt{-C/z} = 1$ and almost zero respectively.

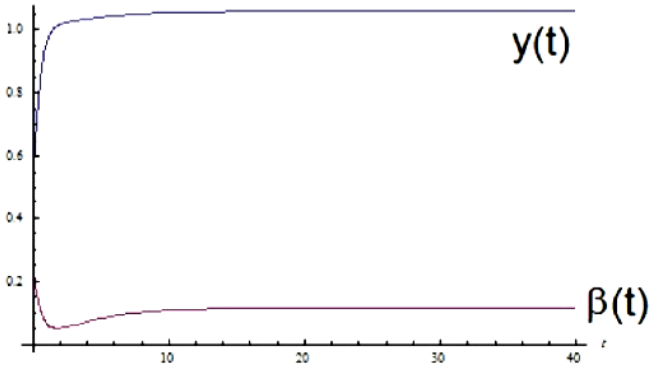

Figure 5. Solutions of the optimal control

REFERENCES

Almog, N., Goldfinger, N., Rotter, V. (2000) p53-dependent apoptosis is regulated by a C-terminally alternatively spliced form of murine p53. *Oncogene.* **19**, 395-403.

Almong, N., Rotter, V. (1997) involvement of p35 in cell differentiation and development. *Biochim. Biopys. Acta,* **1378**, 43-54.

Banin, S., Moyal, L., Shieh, S., Taya, Y., Anderson, C.W., Chessa, L,.Smorodinsky, N.I., Prives, C., Reiss, Y., Shiloh, Y., Ziv, Y. (1998) Enhanced phosphorylation of p53 by ATM in response to DNA damage. *Science*. **281**, 1674-1677.

Bar-Or, R.L., Maya, R., Segel, L.A., Alon, U., Levine, A.J., Oren, M. (2000) Generation of oscillations by the p53-Mdm2 feedback loop: A theoretical and experimental study. *PNAS,* **97**, *no*. 21. 11250–11255.

Chickarmane, V., Ray, A., Sauro, H.M., Nadim, A. (2007), A Model for p53 Dynamics Triggered by DNA Damage*, Siam J. applied dynamical systems,* **6** *no*. 1, 61–78.

Ciliberto, A., Novak, B., Tyson, J.J. (2005) Steady states and oscillations in the p53-Mdm2 network. *CellCycle,* **4**, 107-112.

Guckenheimer, J., Holmes, P. (1993): Nonlinear Oscillations, Dynamical Systems and Bifurcations of Vector Fields, *2nd Edition Springer-Verlag, New York, pp* 117-156.

Hinow, P., Rogers, C.E., Barbieri, C.E., Pietenpol, J.A., Kenworthy, A.K., DiBenedetto, E. (2006) The DNA Binding Activity of p53 Displays Reaction-Diffusion Kinetics. *Biophys. J.,* **91**, 330–342.

Kohn, K.W., Pommier, Y. (2005) Molecular interaction map of the p53 and Mdm2 logic elements, which control the Off–On switch of p53 in response to DNA damage. *Biochem. Biophys. Res. Communic.,* **331**, 816–827.

Ma, L., Wagner, J., Rice, J.J., Hu, W., Levine, A.J., Stolovitzky, G.A. (2005) A plausible model for the digital response of p53 to DNA damage, *Proc. Natl. Acad. Sci USA.,* **102**, 14266-14271.

McCoy, M.A., Gesell, J.J., Mary M. Senior, Daniel F. (2003) Flexible lid to the p53-binding domain of human Mdm2: Implications for p53 regulation. *Proc. Natl. Acad. Sci USA.,* **100**, 1645–1648.

Qi, J.P., Shao, S.H., Xie, J., Zhu, Y. (2007) A mathematical model of P53 gene regulatory networks under radiotherapy. *Biosystems,* **90**, 698–706.

Rabieimotlagh, O., Afsharnezhad, Z. (2010) On the conditions for which the ATM protein can switch off the DNA damage signal in a P53 model, *Studia UBB Biologia,* **55** (1), 67-79.

Sigal, A., Rotter, V. (2000) Oncogenic mutations of the p53 tumor suppressor: the demons of the guardian of the genome. *Cancer Res.,* **60**, 6788-6793.

Wagner, J., Ma, L., Rice, J.J., Hu, W., Levine, A.J., Stolovitzky, G.A. (2005) p53–Mdm2 loop controlled by a balance of its feedback strength and effective dampening using ATM and delayed feedback. *IEE Proc.-Syst. Biol.,* **152**, No. 3. 109-118.

Yan, S., Zhuo, Y. (2006) A unified model for studying DNA damage-induced p53–Mdm2 interaction, *Physica D: Nonlinear Phenomena,* **220** (2), 157–162.

STUDIA UBB BIOLOGIA, LVII, 2, 2012 (p. 71-79)

=== IN MEMORIAM ===

CENTENARUL NAŞTERII PROFESORULUI DR. GEORGE EMIL PALADE (19 noiembrie 1912 – 8 octombrie 2008)

Singurul om de ştiinţă de origine română care a fost distins cu Premiul Nobel în Fiziologie sau Medicină, alături de Albert Claude şi Christian de Duve, **George Emil Palade** s-a născut pe 19 noiembrie 1912, la Iaşi. După propriile spuse, Palade a crescut în mijlocul unei familii de profesori, învăţând să îndrăgească şi să respecte cărţile, să se dedice educaţiei intelectuale. Aşa cum se întâmplă adesea, tânărul George s-a orientat spre o carieră, alta decât cea sperată de tatăl său, profesor de filosofie. Palade a ales să se specializeze în Medicină, la Universitatea din Bucuresti, al cărei student a devenit în anul 1930. Ocolind conformismul şi mânat de curiozitate şi pasiune pentru ştiinţă, studentul medicinist Palade urmează un drum neobişnuit, concentrându-se pe aspecte fundamentale ale ştiinţelor medicale. Anatomia şi histologia l-au interesat în mod deosebit, dedicându-se aproape în totalitate studiului microscopic al ţesuturilor şi celulei. Mai mult, teza sa de doctorat, pe care şi-a susţinut-o în 1940, a abordat un subiect ieşit din tiparele preocupărilor obişnuite ale colegilor de la Medicină: structura nefronului de la delfin (*Delphinus delphi*) în contextul adaptării mamiferelor la viaţa marină. După ce a servit, în calitate de medic, Armata Română, pe durata celui de-al Doilea Război Mondial, doctorul Palade pleacă în S.U.A., în 1946. Încurajat de endocrinologul român Grigore T. Popa, descoperitorul sistemului port hipotalamo-hipofizar (Popa şi Fielding, 1933), Palade a decis să emigreze şi să-şi continue studiile postdoctorale la Universitatea din New York, apoi la Institutul Rockefeller de Cercetări Medicale (în prezent,

Universitatea Rockefeller). Despre acest moment decisiv al carierei sale, Palade spunea într-un interviu acordat publicaţiei Ad Astra în anul 2002: „*Aveam sentimentul că nu ştiu destul, şi că dacă vreau cu adevărat să fac ceva semnificativ trebuie să merg în altă parte – adică în acele locuri unde se desfăşoară activităţi ştiinţifice cu adevărat interesante.*" [Tudor I. Oprea: Interviu cu George Emil Palade, Ad Astra 1(2), 2002]. La New York, Palade a fost atras de posibilitatea colaborării cu profesorul Albert Claude, un cercetător de origine belgiană, faimos deja în toată lumea pentru remarcabilele sale descoperiri biologice făcute cu ajutorul microscopiei electronice. După reîntoarcerea lui Albert Claude în Belgia, perfecţionistul cercetător Palade îşi continuă munca neobosită de optimizare a tehnicilor de microscopie electronică, încercând să obţină preparate microscopice care să permită descrierea cât mai detaliată a organizării tisulare şi celulare. Împreună cu colegii săi din „grupul Rockefeller", George Hogeboom şi Walter Schneider, Palade a fost primul biolog care a apelat la fracţionarea celulară ca etapă esenţială în pregătirea probelor biologice, procedură ce constă în separarea organitelor celulare prin centrifugarea diferenţiată a lizatului celular (Hogeboom şi colab., 1948). Excelent practician, metodic şi inspirat, Palade inovează în laborator, introducând tehnica păstrării intacte a organitelor celulare prin suspendarea lor în soluţie izotonică de zaharoză şi îmbunătăţind procedeul de fixare folosind soluţie de tetraoxid de osmiu tamponată la pH fiziologic (Palade, 1952). George Palade va rămâne la Institutul Rockefeller până în 1973, după care va fi invitat sa preia poziţia de profesor la Facultatea de Medicină a Universităţii din Yale. La Institutul Rockefeller, Palade a lăsat în urmă o puternică şcoală de biologie celulară şi moleculară, unul dintre foştii săi discipoli, Günter Blobel, fiind şi el laureat al Premiului Nobel în Fiziologie sau Medicină (1999) pentru descoperirea secvenţelor-semnal de transport şi localizare a proteinelor (Blobel şi Dobberstein, 1975a; 1975b). După 17 ani petrecuţi la Yale, profesorul de biologie celulară George Emil Palade se va muta la Universitatea California din San Diego, unde a ţinut cursuri în calitate de profesor emerit, până aproape de momentul decesului (7 octombrie 2008).

Considerat de către mulţi, drept unul dintre fondatorii „Biologiei Celulare şi moleculare", Palade are meritul de a fi identificat şi caracterizat, în urma unui efort consecvent, a colaborărilor cu importante nume din domeniile citologiei, histologiei, anatomiei, patologiei celulare, microscopiei şi biochimiei, dar şi printr-o susţinere necondiţionată din partea Institutului Rockefeller, o pleiadă întreagă de de structuri subcelulare. Dintre aceste descoperiri se detaşează cea a particulelor ribonucleoproteice responsabile de biosinteza proteinelor, particule denumite ulterior ribosomi (corpusculii lui Palade), organite abundente în mod special în celule embrionare şi glandulare (Palade, 1955). În afara acestei descoperiri majore, Palade reuşeşte, alături de alţi colaboratori, să descrie ultrastructura mitocondriei (Palade, 1953), a veziculelor sinaptice (Palade şi Palay, 1954), să demonstreze natura artificială a microsomilor (Palade şi Siekevitz, 1956), să caracterizeze procesele de secreţie proteică din celulele pancreatice (Siekevitz şi Palade, 1958a; 1958b; 1958c; 1959; 1960a; 1960b; 1962), să clarifice structura şi rolurile joncţiunilor celulare de la nivelul epiteliilor (Farquhar şi Palade, 1963), să descrie corpusculii Weibel-Palade cu rol în secreţia factorului de coagulare von Willebrand şi a selectinei P din endoteliile vasculare (Weibel şi Palade, 1964), să investigheze biogeneza membranelor tilacoidale (Ohad şi colab., 1967a; 1967b) sau să desluşească organizarea reticulului endoplasmatic (Leskes şi colab., 1971a; 1971b), ca să amintim doar o parte din tabloul impresionantelor sale contribuţii ştiinţifice.

În mod suprinzător, Palade revine în România în 1968, cu prilejul unei vizite oficiale în calitate de membru al delegaţiei Academiei de Ştiinţe a S.U.A. Deşi curtat cu intenţii vădit propagandistice de către conducerea comunistă a ţării, George Emil Palade pune bazele unei reale colaborări cu biologi români. În 1970, Prof. Nicolae Simionescu şi Maya Simionescu au fost invitaţi să lucreze în Laboratorul de Biologie Celulară condus de Palade la Universitatea Rockefeller. Acest parteneriat ştiinţific, care a durat aproape două decenii, se va concretiza printr-o serie de studii ultrastructurale şi fiziopatologice asupra endoteliilor capilare, dar şi cu înfiinţarea, în 1979, a Institutului de Biologie şi Patologie Celulară, la Bucureşti.

În aceeaşi perioadă de deschidere politică şi culturală a României socialiste, profesorul Palade a vizitat şi *Alma Mater Napocensis*. În 1969, a ţinut o conferinţă în amfiteatrul Institutului de Chimie, filială a Academiei Române, iar în luna noiembrie a anului 1971 a revenit la invitaţia Filialei Cluj a Academiei R.S.R. Această din urmă ocazie a prilejuit, în cadrul unei întruniri organizate la Centrul de Cercetări Biologice (C.C.B.), întâlnirea profesorului Palade cu Acad. Emil Pop, Prof. Victor Preda (directorul C.C.B. la acea vreme), Prof. V. Gh. Radu, Prof. Ioan Chiricuţă, Prof. Crişan Mircioiu şi alţii, cel mai apropiat de domeniul de cercetare fiind Dr. Constantin Crăciun, în prezent profesor, director al Centrului de Microscopie Electronică din cadrul Universităţii „Babeş-Bolyai". Dr. Constantin Crăciun, pe atunci având gradul de cercetător ştiinţific în Laboratorul de Biologie Experimentală al C.C.B. Cluj, i-a prezentat rezultatele primelor sale cercetări ultrastructurale privind evoluţia aparatului Golgi în timpul procesului de secreţie muco-proteică din celulele glandulare ale canalului deferent la izopode, cercetare inspirată din lucrările profesorului Palade. Plăcut surprins, George Emil Palade, în interviul acordat prof. Mircioiu (ziarul Faclia din 4.XI.1971) a declarat că a fost „impresionat de calitatea microscopiei electronice a dr. Crăciun" şi a comunicat intenţia de a-l sprijini în vederea acordării unei burse în laboratorul de microscopie electronică de la Institutul Rockefeller din New York.

În continuare, Prof. Constantin Crăciun rememorează o întâmplare savuroasă petrecută cu ocazia acelei vizite, dar şi alte amintiri legate de personalitatea profesorului Palade:

„A doua zi [după întâlnirea de la C.C.B., *n.a.*], profesorul Palade avea de susţinut două conferinţe în aula Institutului de Chimie al Academiei, ocazie cu care m-a rugat să îl ajut cu proiectarea diapozitivelor conferinţei, dar, surpriză, diapozitivele sale erau pe plăci de sticlă de 9 x 12 cm, ceea ce m-a pus la grea încercare. Am reuşit să găsesc în pod la Facultatea de Geografie un aparat de proiecţie, dar fără rame de pus diapozitive, însă, cu ajutorul tâmplarului de aici, s-au confecţionat ramele respective. După conferinţe, profesorul Palade, văzând ramele din lemn şi povestindu-i întâmplarea, a exclamat: „*Doamne, mintea românului!*". La întrunirea de la C.C.B., domnul

Palade ne-a mai declarat: „*Eu i-am extras pe soţii Simionescu din România şi acum lucrăm împreună*". Ulterior, i-am trimis felicitări cu ocazia primirii Premiului Nobel. Prin anul 2000, i-am trimis poştal câte un exemplar din revista noastră de biologie celulară [Analele Societăţii Naţionale de Biologie Celulară, *n.a.*]. În iunie 2003, i-am scris personal cu referire la acordarea domniei sale, de către U.B.B., a distincţiei de „Doctor Honoris Causa", împreună cu Günter Blobel şi Bhanu P. Jena, la care mi-a răspuns cu o scrisoare de mulţumire. În noiembrie 2003, am fost invitat împreună cu Prof. Gheorghe Benga, cu ocazia celebrării împlinirii vârstei de 90 ani a profesorului Palade, la Wayne State University, din Detroit, prilej cu care s-a instituit premiul internaţional dotat cu medalia de aur „George Emil Palade", iar universitatea respectivă din Detroit a luat numele de „George Palade University". Atunci, prima medalie de aur i-a fost atribuită lui Günter Blobel, discipol de-al lui Palade, el însuşi laureat al Premiului Nobel pentru medicină în 1999. În decembrie 2008, cu ocazia primirii de către mine a distincţiei „Doctor Honoris Causa" acordată de U.M.F. Cluj-Napoca, am închinat expunerea mea Prof. George Emil Palade, iar în octombrie 2011, la "The First World Congress on Water Channel Proteins" am prezentat expunerea "Impressions from attending in November 2003 in Detroit, U.S.A. the first "George Emil Palade" lecture and award of the "George Emil Palade" Gold Medal to Günter Blobel (1999 Nobel Laureate in Physiology or Medicine)". În anul 2011, a apărut cartea *Mica enciclopedie de mari valori ridicate dintre români*, în care, împreună cu Prof. Corneliu Tarba, am scris medalionul despre viaţa şi activitatea savantului George Emil Palade. În luna martie 2013 va apărea, la editura Risoprint Cluj-Napoca, o ediţie îmbunătăţită a acestui volum, în limba engleză, *The Encyclopedia of Outstanding Romanian Personalities*, care va fi lansată la Târgul Inventică pe 19 martie, la Expo Transilvania. Pentru tot ce am scris mai sus am documente scrise însoţite de fotografii personale, inclusiv fotografia făcută de mine în 1971 profesorului Palade în timpul conferinţei de la Chimie" (vezi imaginea de mai jos).

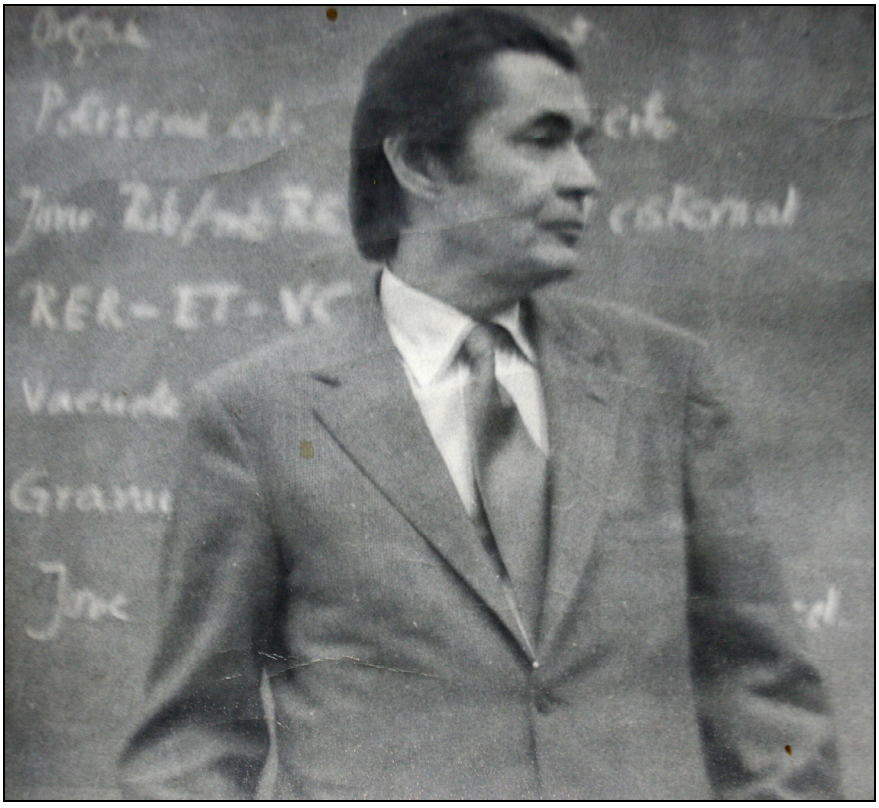

Imagine: *Profesorul G.E. Palade conferenţiind la Institutul de Chimie al Academiei Române din Cluj-Napoca despre căile de secreţie ale proteinelor în celulele pancreatice (noiembrie, 1971)*

(Sursa: Arhiva de Fotografii a Centrului de Microscopie Electronică, Universitatea "Babeş-Bolyai" din Cluj-Napoca).

Pe lângă Premiul Nobel obţinut în 1974, Palade a mai fost onorat cu o serie de distincţii, dintre care amintim premiul Fundaţiei Albert Lasker (1966). A primit titlul de membru al Academiei de Ştiinţe a S.U.A., în 1961, iar în 1986 i s-a acordat Medalia Naţională pentru Ştiinţă de către preşedintele Ronald Reagan. În 1976, a fost numit preşedinte al Asociaţiei Americane de Biologie Celulară (The American Society for Cel Biology - ASCB), postură

onorantă de care s-au mai bucurat, printre alţii: Marc Kirschner (1991), J. Michael Bishop (1996), Harvey Lodish (2004) sau Bruce Alberts (2007). Pe plan naţional, meritele sale au fost recunoscute prin dobândirea calităţii de membru al Academiei Române (1975) şi prin decorarea, în 2007, cu Ordinul Naţional Steaua României în grad de Colan, cea mai importantă distincţie a statului român.

Horia Banciu

Departamentul de Biologie Moleculară şi Biotehnologie
Facultatea de Biologie şi Geologie
Universitatea "Babeş-Bolyai" din Cluj-Napoca

BIBLIOGRAFIE

Blobel, G., Dobberstein, B.T. (1975a) Transfer of proteins across membranes. I. Presence of proteolytically processed and unprocessed nascent immunoglobulin light chains on membrane-bound ribosomes of murine myeloma. *J Cell Biol.*, **67** (3): 835–851.

Blobel, G., Dobberstein, B.T. (1975b) Transfer to proteins across membranes. II. Reconstitution of functional rough microsomes from heterologous components. *J Cell Biol.*, **67** (3): 852–862.

Farquhar, M.G., Palade, G.E. (1963) Junctional complexes in various epithelia. *J. Cell Biol.*, **17**: 375-412

Hogeboom, G.H., Schneider, W.C., Pallade, G.E. (1948) Cytochemical studies of mammalian tissues. I. Isolation of intact mitochondria from rat liver; some biochemical properties of mitochondria and submicroscopic particulate material. *J. Biol. Chem.*, **172** (2): 619-635

Leskes, A., Siekevitz, P., Palade, G.E. (1971a) Differentiation of endoplasmic reticulum in hepatocytes: I. Glucose-6-Phosphatase Distribution *in situ*. *J. Cell Biol.* **49** (2): 264-287.

Leskes, A., Siekevitz, P., Palade, G.E. (1971b) Differentiation of endoplasmic reticulum in hepatocytes: II. Glucose-6-Phosphatase in Rough Microsomes. *J. Cell Biol.* **49** (2): 288-302.

Ohad, I., Siekevitz, P., Palade, G.E. (1967a) Biogenesis of chloroplast membranes. I. Plastid dedifferentiation in a dark-grown algal mutant (*Chlamydomonas reinhardi*). *J. Cell Biol.*, **35** (3):521-552.

Ohad, I., Siekevitz, P., Palade, G.E. (1967b) Biogenesis of chloroplast membranes. II. Plastid Differentiation during Greening of a Dark-Grown Algal Mutant (*Chlamydomonas reinhardi*). *J. Cell Biol.*, **35** (3):553-584.

Palade, G.E. (1952) A study of fixation for electron microscopy. *J. Exp. Med.*, **95** (3): 285–298.

Palade, G.E. (1953) An electron microscope study of the mitochondrial structure. *J. Histochem. Cytochem*., **1** (4): 188–211.

Palade, G.E. (1955) A small particulate component of the cytoplasm. *J. Biophys. Biochem. Cytol*., **1** (1): 59-68.

Palade, G.E., Palay, S.L. (1954) Electron microscope observations of interneuronal and neuromuscular synapses. *Anat. Rec.*, **118**: 335–336.

Palade, G.E., Siekevitz, P. (1956) Liver microsomes; an integrated morphological and biochemical study. *J. Biophys. Biochem. Cytol.*, **2** (2): 171-200.

Popa, G.T., Fielding, U. (1933) Hypophysio-Portal vessels and their colloid accompaniment. *J Anat.*, **67** (Pt 2): 227–232.

Siekevitz, P., Palade, G.E. (1958a) A cytochemical study on the pancreas of the guinea pig. I. Isolation and enzymatic activities of cell fractions. *J. Biophys. Biochem. Cytol*., **4** (2): 203-218.

Siekevitz, P., Palade, G.E. (1958b) A cytochemical study on the pancreas of the guinea pig. II. Functional variations in the enzymatic activity of microsomes *J. Biophys. Biochem. Cytol*., **4** (3): 309-318.

Siekevitz, P., Palade, G.E. (1958c) A cyto-chemical study on the pancreas of the guinea pig. III. In vivo incorporation of leucine-1-C14 into the proteins of cell fractions. *J. Biophys. Biochem. Cytol*., **4** (5): 557-566.

Siekevitz, P., Palade, G.E. (1959) A cytochemical study on the pancreas of the guinea pig. IV. Chemical and metabolic investigation of the ribonucleoprotein particles. *J. Biophys. Biochem. Cytol*., **5** (1): 1-10.

Siekevitz, P., Palade, G.E. (1960a) A cytochemical study on the pancreas of the guinea pig. V. In vivo incorporation of leucine-1-C14 into the chymotrypsinogen of various cell fractions. *J. Biophys. Biochem. Cytol*., **7** (4): 619-630.

Siekevitz, P., Palade, G.E. (1960b) A cytochemical study on the pancreas of the guinea pig. VI. Release of enzymes and ribonucleic acid from ribonucleoprotein particles. *J. Biophys. Biochem. Cytol*., **7** (4): 631-644.

Siekevitz, P., Palade, G.E. (1962) Cytochemical study on the pancreas of the guinea pig. VII. Effects of spermine on ribosomes. *J. Biophys. Biochem. Cytol*., **13**: 217-232.

Weibel, E.R., Palade, G.E. (1964). New cytoplasmic components in arterial endothelia. *J. Cell Biol.*, **23** (1): 101–112.

*** "George E. Palade – Autobiography". Nobel Lectures, Physiology or Medicine 1971-1980, (Lindsten, J., Ed.), World Scientific Publishing Co., Singapore, 1992.

*** "George E. Palade - Nobel Lecture: Intracellular Aspects of the Process of Protein Secretion", Nobel Lectures, Physiology or Medicine 1971-1980 (Lindsten, J., Ed.), World Scientific Publishing Co., Singapore, 1992.

*** "Tudor I. Oprea: Interviu cu George Emil Palade", Ad Astra **1** (2), 2002, http://www.ad-astra.ro/journal/2/interview_palade_ro.pdf

*** Mică enciclopedie de mari valori ridicate dintre români (Bărglăzan, M., Borcilă, M., Crudu, D., Căpăţână, O., Crăciun, C., editori), Imprimeria Ardealul, Cluj-Napoca, 2011.

*** The Encyclopedia of Outstanding Romanian Personalities (Căpăţână, O., coordonator), Ed. Risoprint, Cluj-Napoca, 2013.

STUDIA UBB BIOLOGIA, LVII, 2, 2012 (p. 81-82)

=== BOOK REVIEW ===

ECOLOGICAL AND BEHAVIORAL METHODS FOR THE STUDY OF BATS, 2ND EDITION

ENDRE JAKAB[1, 2]

Ecological and Behavioral Methods for the Study of Bats, 2nd edition. Edited by Thomas H. Kunz and Stuart Parsons, Johns Hopkins University Press, Baltimore, 2009, xviii + 901 p. ISBN: 978-0-8018-9147-2

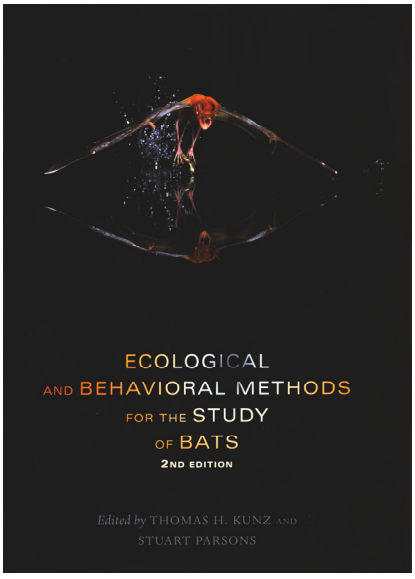

Appeared after twenty-one years from the first edition the *second edition* of the *Ecological and Behavioral Methods for the Study of Bats* could be considered a primary reference for bat biologists. It is a complete guide not only for beginners but also for professional bat researchers. Edited by professor Thomas H. Kunz from Boston University, USA and bioacoustics specialist Stuart Parsons, associate professor at University of Auckland, New Zealand, this book contains comprehensive reviews written by 84 contributors from all over the world.

[1] *Hungarian Department of Biology and Ecology, Faculty of Biology and Geology, Babeş-Bolyai University, 5-7 Clinicilor st., 400006 Cluj-Napoca, Romania, ejakab@hasdeu.ubbcluj.ro*
[2] *Molecular Biology Center, Interdisciplinary Research Institute in Bio-Nano-Sciences, Babeş-Bolyai University,42. August Treboniu Laurian st., 400271 Cluj-Napoca, Romania.*

It is organized into eleven parts, each of them containing several chapters. Parts I to III cover methods for capturing, handling and marking bats, using conventional field techniques (such as mist netting, harp traps and use of banding devices), new radiotelemetry techniques and non-invasive ultrasonic detection methods, as well as methods for assessing colony size, prenatal and postnatal growth and development in bats, and methods for age estimation and senescence of bats.

Parts IV and V describe useful methods for studying bats in captivity as well as techniques for analysing bat morphology and migration. The following parts cover the effects of environmental contaminants, techniques for measuring milk composition in small bats (part VI), food habits analysis and nutritional ecology aspects (part VII) as well as thermal biology of bats (part VIII).

The last chapters of the book are focused on phylogenetic tools for examining evolution of bats, phylogeographic analysis of bats (part IX), methods for assessing diseases in bats and public health concerns (part X), as well as methods that promote bat conservation and a list of bat themed educational resources (part XI).

Finally I would like to thank to Carolyn Birch from Oxford Publicity Partnership Ltd. and to The Johns Hopkins University Press providing me the inspection copy of this book.